Sadraque Silva Viana

On the Use of Signal Processing Techniques for Single-trial P300 Detection

Belo Horizonte

August, 2017

Sadraque Silva Viana

On the Use of Signal Processing Techniques for Single-trial P300 Detection

Dissertation presented to the Graduation Course in Electrical Engineering of Universidade Federal de Minas Gerais as a partial requirement for obtaining the degree of Master's in Electrical Engineering.

Universidade Federal de Minas Gerais

School of Engineering

Graduation Program in Electrical Engineering

Advisor: Dr. Danilo Barbosa Melges, DEE/UFMG

Co-Advisor: Dra. Paula Luciana Scalzo, DMOR/UFMG

Belo Horizonte

August, 2017

Sadraque Silva Viana
On the Use of Signal Processing Techniques for Single-trial P300 Detection/ Sadraque Silva Viana. – Belo Horizonte, August, 2017-
91 p. : il. (some in color) ; 30 cm.

Advisor: Dr. Danilo Barbosa Melges, DEE/UFMG

Master's Dissertation – Universidade Federal de Minas Gerais
School of Engineering
Graduation Program in Electrical Engineering , August, 2017.

1. P300. 2. Single-trial detection. 3. Brain-computer interface. I. Universidade Federal de Minas Gerais. II. School of Engineering. III. Graduation Program in Electrical Engineering. IV. On the Use of Signal Processing Techniques for Single-trial P300 Detection.

Sadraque Silva Viana

On the Use of Signal Processing Techniques for Single-trial P300 Detection

Dissertation presented to the Graduation Course in Electrical Engineering of Universidade Federal de Minas Gerais as a partial requirement for obtaining the degree of Master's in Electrical Engineering.

Dissertation approved. Belo Horizonte, August 23th, 2017:

Dr. Danilo Barbosa Melges,
DEE/UFMG
Advisor

Dra. Paula Luciana Scalzo,
DMOR/UFMG
Co-Advisor

Prof. Dr. Eduardo Mazoni Andrade Marçal Mendes

Prof. Dr. Andre Paim Lemos

Belo Horizonte

August, 2017

To my thirteen year old Self:
You never thought You would arrive here!".

Acknowledgements

To Life itself and the possibility of Existence: for if I am granted to Be, it is my duty to love and to learn.

To being capable of experiencing the Good and the Bad, the Memorable and the Forgettable, the Astonishing and the Uneventful: to all of this, I'm truly grateful.

To Whom I was: for raising me to be who I am.

To my family and friends: this is where all those weekends have gone to waste.

To my girlfriend, Ana: thanks for joining me in this ride, and many more yet to come.

To my advisor, Danilo Melges: for uncountable hours of "philosophical discussions".

To all the human beings who have once been, currently are or someday will become part of my Existence, excuse me for repeating myself, however, to this very moment of my life, this is the best model I can come up with: my friends, it does not matter which events have made us resentful. Lest we not forget that we are capable of love and that, one day, joy shall define all of our endeavors. Do not mourn or suffer with the passage of time; it bears rememberance that, however humble our beginnings, we too shall find peace.

Thank you all.

"Não há nada mais belo
do que a oportunidade
de escrever diariamente
os versos que compõem
a poesia da própria vida.
(Sadraque Viana, Poema das Semanas Felizes)

"Peut-être l'immobilité des choses autour de nous leur est-elle imposée par notre certitude que ce sont elles et non pas d'autres, par l'immobilité de notre pensée en face d'elles. (Marcel Proust, Du côté de chez Swann, p.12)

Abstract

P300 is an event-related potential (ERP) recorded in the scalp using electroencephalography (EEG), commonly employed in the development of brain-computer interfaces (BCI). This potential presents low signal-to-noise ratio (SNR), which makes the detection of such signal a very difficult task. To overcome the low SNR, a technique known as coherent average is commonly used. However, it requires longer EEG recording in order to average a high number of stimuli-synchronized EEG windows, making it difficult to implement P300-based BCI. Hence, techniques that can effectively perform single-trial P300 detection (using only one stimulus) have been investigated to enhance the performance of such systems. In this dissertation, four signal processing techniques (Independent Component Analysis, Time and Frequency Extracted Parameters, Variance-Based Metrics, Wavelet Coefficients) are used to generate relevant EEG features and three classifiers (Logistic Classifiers, Linear Discriminant Analysis, Support Vector Machines) were applied to perform single-trial P300 detection. Data from three different databases, containing EEG signals recorded during a P300-speller usage, were employed to validate the techniques. Two of them contained signals collected from healthy subjects and the other one was composed of signals recorded from Amyotrophic Lateral Sclerosis (ALS) patients. The performance of the combinations of signal processing techniques and classifiers was evaluated by comparing accuracy, sensitivity, specificity and area under the ROC curve and by applying the Friedman test to verify if there are statistically significant differences. The best results achieved mean accuracies of 84.0 $\pm$ 4.2% for healthy subjects and 71.5 $\pm$ 1.6% for ALS diagnosed subjects, showing that the studied methods are promising for single-trial BCI implementation. Among the signal processing techniques, Independent Component Analysis performed better for one database (healthy subjects), while Variance-Based Metrics obtained better results for the two other databases.

Keywords: P300, Independent Component Analysis, Discrete Wavelet Transform, Logistic Classifier, Linear Discriminant Analysis, Support Vector Machines, Brain-Computer Interfaces, Virtual Speller, Amyotrophic Lateral Sclerosis.

Resumo

O P300 é um potencial relacionado a evento medido por meio da eletroencefalografia (EEG) e comumente empregado no desenvolvimento de interfaces cérebro-máquina (ICM). Este potencial apresenta baixa razão sinal-ruído (RSR), o que torna sua detecção uma tarefa bastante difícil. Para superar a baixa RSR, utiliza-se uma técnica conhecida como média coerente. Entretanto, esta técnica requer períodos de medição de EEG mais longos, de modo a realizar a média de elevada quantidade de janelas sincronizadas com o estímulo, dificultando a implementação de ICM baseadas no P300. Por este motivo, métodos que realizam detecção single-trial (com somente um estímulo) deste potencial vem sendo investigadas para melhorar o desempenho destes sistemas. Nesta dissertação, quatro técnicas de processamento de sinais (Análise de Componentes Independentes, Parâmetros Extraídos no Tempo e Frequência, Métrica Baseada em Variância e Transformada Discreta de Wavelet) foram usadas para extrair características relevantes dos sinais de EEG e três classificadores (Classificador Logístico, Análise Discriminante Linear, Máquina de Vetores de Suporte) foram empregados para realizar detecção single-trial do P300. Foram utilizadas três bases de dados contendo sinais de EEG coletados durante o uso de um soletrador virtual (P300-speller). Duas das bases de dados são compostas de sinais de voluntários saudáveis e a outra de pacientes de Esclerose Lateral Amiotrófica (ELA). O desempenho das combinações de técnicas de processamento e classificadores foi avaliado comparando-se a acurácia, a sensibilidade, a especificidade e a área abaixo da curva ROC, sendo aplicado o Teste de Friedman para verificar a existência de diferença estatística significativa. Os melhores resultados alcançaram acurácia média de 84,0 $\pm$ 4,2% para voluntários saudáveis e 71.5 $\pm$ 1.6% para voluntários diagnosticados com ELA, indicando que os métodos são promissores na construção de ICM single –trial. Dentre as técnicas de processamento, a Análise de Componentes Independentes provou-se melhor para uma base de dados (de voluntários saudáveis), enquanto a Métrica Baseada em Variância obteve melhores resultados para as duas outras bases.

Palavras chave: P300, Análise de Componentes Independentes, Transformada Discreta de Wavelet, Classificador Logístico, Análise Discriminante Linear, Máquina de Vetores de Suporte, Interface Cérebro-Máquina, Soletrador Virtual, Esclerose Lateral Amiotrófica.

List of Figures

List of Tables

List of abbreviations and acronyms

ALS	Amyotrophic Lateral Sclerosis
BCI	Brain-Computer Interfaces
ERP	Event-Related Potential
EEG	Electroencephalogram
SNR	Signal-to-Noise Ratio
EEG	Electroencephalogram
ECG	Electrocardiogram
EOG	Electrooculogram
RCP	Row-Column Paradigm
PET	Positron Emission Tomography
fMRI	Functional Magnetic Resonance Imaging
fNIRS	Functional Near-Infrared Spectroscopy
ITR	Information Transfer Rate
VEP	Visual Evoked Potential
PCA	Principal Component Analysis
FLDA	Fisher's Linear Discriminant Analysis
ICA	Independent Component Analysis
CAR	Common Average Reference
TFE	Time and Frequency Extractions
VBM	Variance-Based Metrics
WAV	Wavelet Coefficients
ICA	Independent Component Analysis
LOG	Logistic Classifiers

LDA	Linear Discriminant Analysis
SVM	Support Vector Machines

Contents

1 Introduction

In this chapter, the motivation of the dissertation is presented, along with the objectives of the work and organization of the text.

Various neurological diseases such as stroke, spinal cord injury, cerebral palsy, multiple sclerosis, muscular dystrophy and amyotrophic lateral sclerosis (ALS) can severely damage the neural pathways used to control muscles leading to a critical clinical condition (WOLPAW *et al.*, 2002).

ALS is a neurodegenerative disease that affects primarily the motor system. As the disease advances, a progressive and cumulative disability is observed in patients, leading to eventual death due to failure of respiratory muscles (OLIVEIRA; PEREIRA, 2009).

In order to overcome these disabilities, as well as other types of neurodegenerative diseases such as Parkinson's (HWANG; KWON; IM, 2009), there is a growing interest in brain-computer interfaces (BCI) research.

BCI are systems that can provide alternative means of communication to the peripheral nerves and somatic muscles, allowing the user to control the environment using only brain waves (WOLPAW *et al.*, 2002). A common type of BCI is based on P300, which is an event-related potential (ERP) – electric potentials that arise in the brain as a response to external stimuli – recorded by means of electroencephalographic (EEG) signals, which corresponds to the temporo-spatial sum of electrical potentials in the scalp (DIETRICH; KANSO, 2010).

The P300 arises as a response to sensory stimuli of interest (visual, auditory or somatosensory) that are presented in an infrequent way (*target signals*), alternating with other unimportant stimuli that happen frequently (*non-target signals*) (ALLISON; PINEDA, 2003). This potential is registered most prominently in the centro-parietal region and has a positive peak at around 300ms post-stimulus (ALLISON; PINEDA, 2003). An example of a P300 signal with excellent signal-to-noise ratio (SNR) is shown in Figure 1.1 (solid line), where 120 epochs (an epoch corresponds to an EEG window after the occurrence of a stimulus) were used in the grand average calculation.

P300-based BCI are a very useful alternative for patients whose motor disabilities prevent the use of other biosignals which have better SNR. This is the main motivation why P300-based BCI have been the objective of intensive research (WOLPAW *et al.*, 2002; BASHASHATI *et al.*, 2007; MCFARLAND *et al.*, 2011; MAGEE; GIVIGI, 2015a).

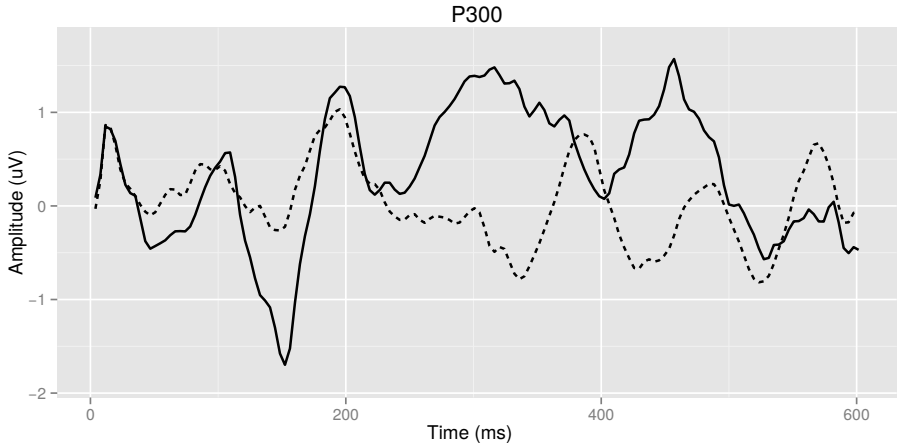

Figure 1.1 – Example of P300 potential with good SNR. The solid line contains the elicited P300; the dashed line contains spontaneous EEG.

However, detecting P300 is a very difficult task, as the spontaneuous brain activity (spontaneous or background EEG) masks the P300, as evidenced in Figure 1.2. This figure contains a P300 potential example (solid line) and spontaneous activity example (dashed line). One can notice how it is extremely difficult to visually distinguish between the two classes of signals.

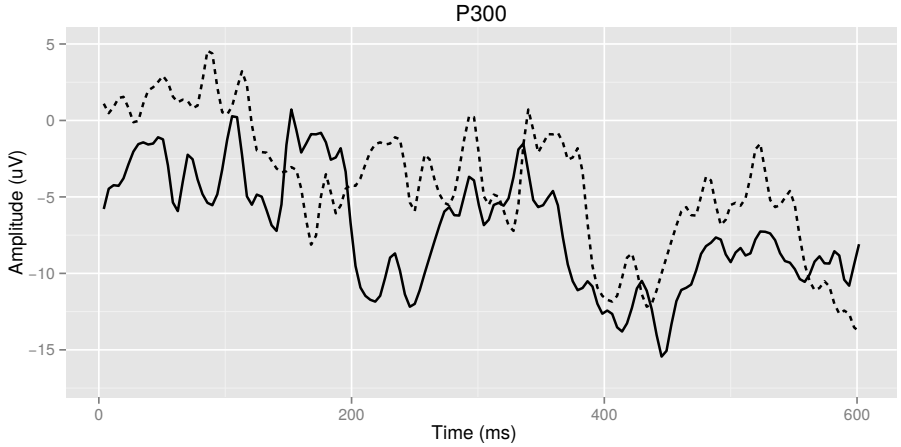

Figure 1.2 – Example of common P300 potential. The solid line contains the elicited P300; the dashed line contains spontaneous EEG.

In order to overcome this obstacle, different signal processing techniques have been employed to remove artifacts, increase the SNR and extract relevant characteristics (MASON; BIRCH, 2003) such as the recent work of Morales *et al.* (2014), Xie *et al.* (2014), Magee e Givigi (2015a).

One of the most common techniques is the grand average, which calculates the average of different EEG epochs and distinct derivations (EEG channels), synchronized

from the instant of stimulation. The grand average reduces the magnitude of the background EEG, thereby increasing the SNR of the P300 estimate and leading to higher classification rates. However, the use of many EEG epochs to calculate the grand average requires longer time intervals to detect the potential, making the implementation of P300-based BCI difficult for practical purposes.

In this context, the focus of this dissertation is to investigate signal processing techniques that are capable of detecting the P300 potential using a small number of EEG epochs, preferably with only one epoch, generally referred in the literature as *single-trial* detection or *single-trial* classification. To accomplish this, one of the most common BCI, known as P300 Speller, composed of an array of alphanumeric characters that are randomly flashed to stimulate the user, will be employed.

Moreover, this work investigates time and frequency characteristics that can further differentiate between *target* (EEG signals that contain P300 potential) and *non-target* (EEG signals that do not contain P300) signals, in order to increase detection rates.

Four signal processing techniques will be employed to generate such characteristics: Independent Component Analysis (ICA), Time and Frequency Extracted Parameters (TFE), Variance-Based Metrics (VBM) and Discrete Wavelet Transforms (WAV).

Using the selected signal characteristics, the performance of three different classification methods will be then compared: Logistic Classifiers (LOG), Linear Discriminant Analysis (LDA) and Support Vector Machines (SVM).

1.1 Objectives

The main objective of this dissertation is to investigate four signal processing techniques for feature extraction and three classification methods that can perform P300 detection masked by spontaneous EEG, using only one trial. All different combination of signal processing techniques and classification methods will be compared and their performances evaluated.

1.2 Organization

This dissertation is organized as follows. The present chapter introduces the motivation and the objectives of this work.

Chapter 2 presents a brief review about electroencephalography and event-related potentials, discussing topics such as EEG acquisition, different types of ERP and P300

eliciation.

Brain-computer interfaces and a review of signal processing techniques used to detect ERP are presented in Chapter 3, which also includes a detailed review of single-trial P300 detection literature.

Chapter 4 presents an in-depth description of the main signal processing techniques and classification methods used in this dissertation, with detailed mathematical formulation.

The methodology employed in this work is described in Chapter 5, from the used databases to the statistical tests applied for performance evaluation.

Chapter 6 summarizes the results of the dissertation, which are then discussed and compared with literature results in Chapter 7.

Finally, the concluding remarks, as well as future work suggestions, are exposed in Chapter 8.

2 Electroencephalography and Event-Related Potentials

This chapter introduces fundamental aspects about electroencephalography, event-related potentials and the P300 potential.

2.1 Spontaneous Electroencephalogram

This section discusses important aspects about EEG characteristics, the signal acquisition, as well as about EEG contamination by artifacts and alternatives to minimize their effects.

2.1.1 Electroencephalography

Electroencephalography is a non-invasive technique that records electrical signals at the scalp using surface electrodes. Such signals results from ionic currents generated by brain neurons' activity filtered by structures like meninges, bones of the skull and skin, leading to the electroencephalogram (EEG) (DIETRICH; KANSO, 2010).

Since such ionic currents are strongly attenuated by these tissues, EEG amplitude is very small (achieving only about 100 μV). Therefore, EEG recording equipment is commonly composed by high-gain precision amplifiers, enabling the acquisition of brain signals (TEPLAN, 2002).

In practice, EEG works like a record of the spatiotemporal sum of electrical signals generated from postsynaptic potentials of the encephalic neurons (DIETRICH; KANSO, 2010).

The average EEG amplitude is 100 μV, with frequency content ranging from 0.1 to 100 Hz. Commonly, the EEG is divided into five frequency bands ((NIEDERMEYER; SILVA, 2004)), illustrated in Figure 2.1.

The *delta* band (0.1 to 3.5 Hz) presents the highest EEG amplitudes and is predominant in children and adults in deep sleep stage. *Theta* activity (4 to 7.5 Hz) is found in light sleep stage and also waking (NIEDERMEYER; SILVA, 2004).

The *gamma* band ($>$ 30 Hz) is observed in different behavioral and experimental conditions, involving sensory and/or cognitive processing. The first records of this EEG band was due to the advent of digital electroencephalography equipment, in 1964, which

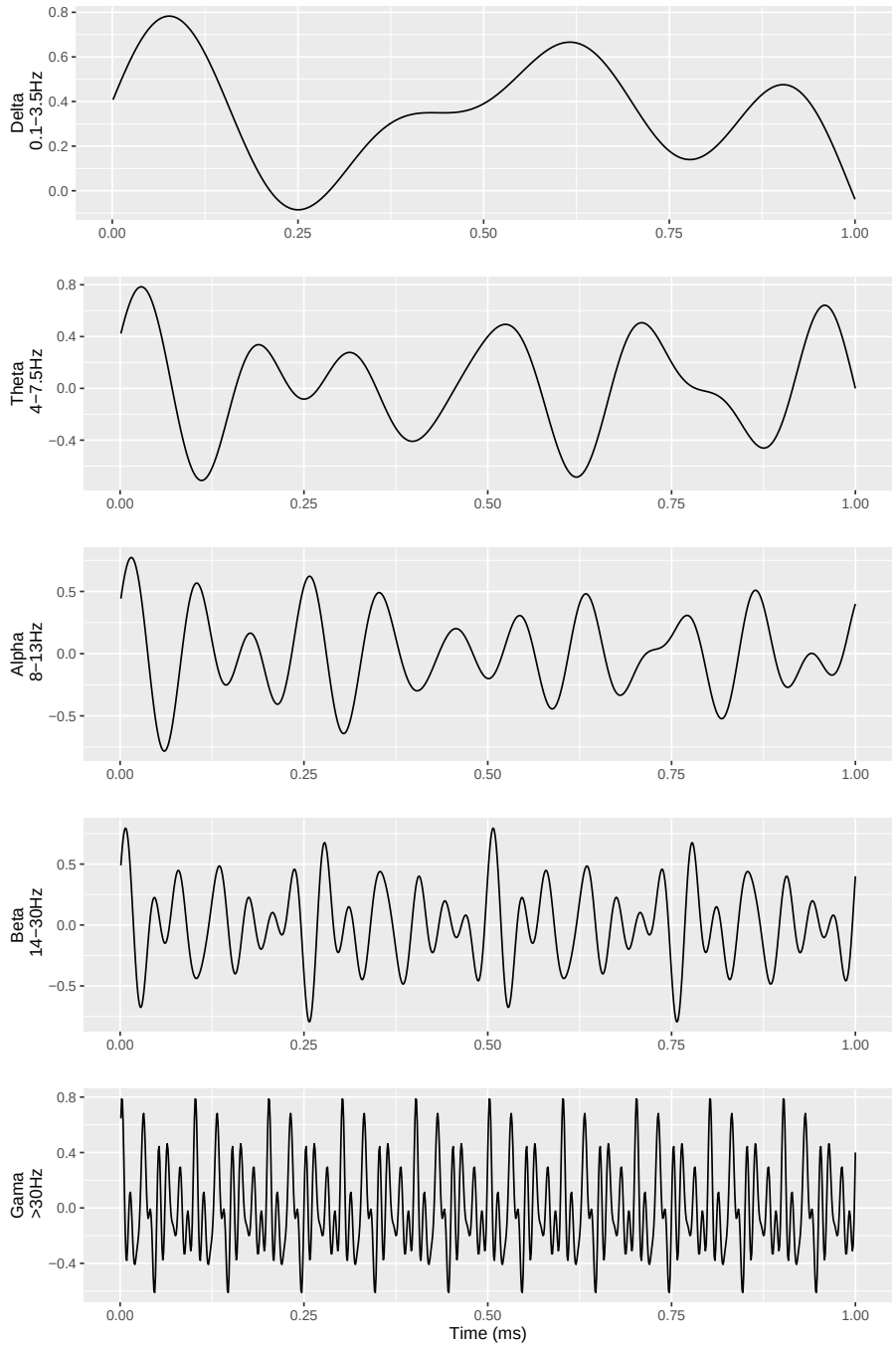

Figure 2.1 – Frequency bands of a real EEG recording.

allowed recording frequencies higher than 25 Hz, different from the conventional analog EEG equipment available at that time (HUGHES, 2008).

Best observed in the posterior regions of the scalp, the *alpha* rhythm (8 to 13 Hz) amplitudes are in the range of 50 μV. When the eyes are closed and a person stay relaxed, the amplitude of this rhythm increases. However, with eyes opened and during alertness or some kind of cognitive task (e.g.: performing a calculation), the amplitude of *alpha*

band is reduced (NIEDERMEYER; SILVA, 2004).

Similar to the *gamma* band, *beta* activity (14 to 30 Hz) has been observed in different experimental conditions and usually has lower amplitude than 30μ V (TEPLAN, 2002). It is mainly associated with brain activities that reflect emotional and cognitive processes (ROWLAND *et al.*, 1985; HERRMANN; MUNK; ENGEL, 2004).

All these frequency bands are present in spontaneous EEG (or background EEG), which is recorded in a condition of non-stimulation. In general, spontaneous EEG does not show any easily recognizable waveform pattern as other biosignals (*e.g.*: electrocardiogram (ECG) QRS complex), hence constituting a random signal, which can only be characterized by its probability density function and its statistical properties.

Although this fact hinders the visual inspection of such signal, the EEG is widely useful in the fields of neurophysiology and clinical neurology. In most applications, signal processing techniques are employed to facilitate interpretation and provide usefull information for specialists.

2.1.2 International 10-20 System

Electroencephalogram signals are typically recorded using the International 10–20 System, depicted in Figure 2.2. This system, initially proposed by Jasper (1958), establishes a standard by which the EEG electrodes are positioned in the scalp, ensuring the reproducibility of EEG records.

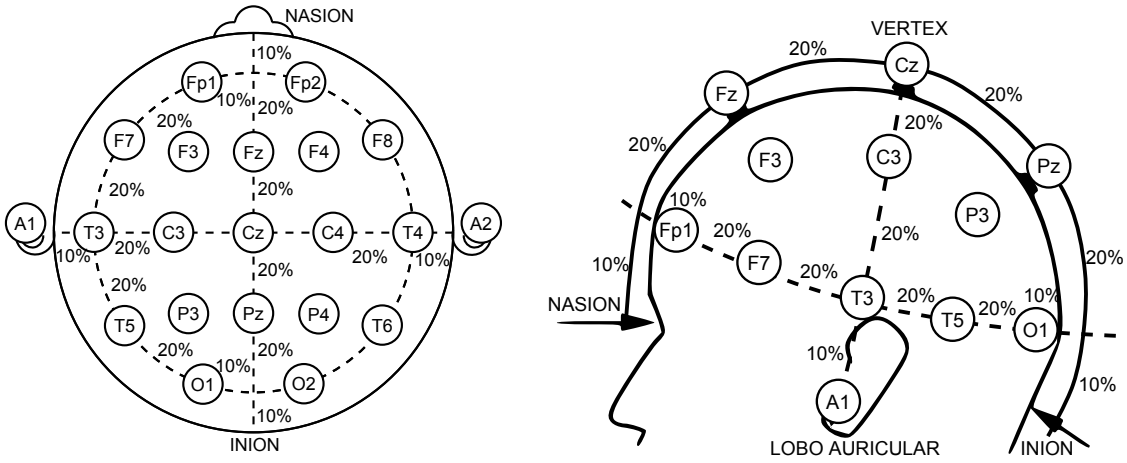

(a) Vista do topo (b) Vista lateral

Figure 2.2 – International 10-20 System for EEG electrodes positioning. Adapted from: <en.wikipedia.org> and (NIEDERMEYER; SILVA, 2004)

According to this system, 21 electrodes are placed on the scalp, distributed using the following anatomical references: the *nasion*, which is located above the nose depression,

and the *inion*, which is a bony protuberance located at the back of the skull, above the *foramen magnum*.

The electrodes are positioned at intervals of 10 and 20% of the *nasion-inion* distance, in mid-sagittal and transverse planes. They are also positioned at the same percent intervals of the distance between earlobes.

Each derivation is named with a letter and a number. The letters identify the following regions: frontopolar (Fp), frontal (F), central (C), temporal (T), parietal (P), occipital (O), and auricular (A). The derivations located on the midline are designated with the letter "Z". Even numbers indicate right hemisphere, and odd numbers indicate left hemisphere (NIEDERMEYER; SILVA, 2004).

2.1.3 Artifacts

EEG records are corrupted by the presence of other electrical signals from various sources. In general, noise added to the EEG by these sources, interfering in the EEG record, is called an artifact. According to their origin, artifacts can be classified into three categories: external, instrumental and physiological (SAUNDERS, 1979).

External artifacts are caused by sources that are not directly involved in the EEG acquisition, but which nevertheless are present in the environment. Klass (1995) cites the following examples of artifacts: interference from power lines, such as electromagnetic noise coming from the electrical network's fundamental and harmonics; equipment connected to the patient, such as ventilators; other equipment that is often present in the environment, such as lamps, heaters and air conditioners. Extrinsic artifacts are generally dealt with using shielding.

When the equipment used to perform electroencephalography is the source of noise in the EEG record, the interference is called an instrumental artifact. Such is the case when there is malfunction of electrodes or their connections, amplifiers, switches and oscillators (KLASS, 1995).

The physiological artifacts are among the most common ones and their sources include involuntary muscle movements, electrocardiogram, electrooculogram (EOG) and even spontaneous movements of the patient. The EOG deserves special mention, since its origin is very close to the electrodes used to record the EEG. While EEG presents amplitudes around tens of microvolts, ECG and EOG have magnitudes of the order of millivolts, and therefore it can strongly distort the recorded EEG signal (NOLAN; WHELAN; REILLY, 2010).

Special attention to the equipment setup, environment and experimental protocol is required to minimize the impact of artifacts in the EEG records. However, artifacts will still be present in the acquired signals. Due to this reason, artifact removal techniques are employed as a pre-processing step.

2.2 Event-Related Potentials (ERP)

This section introduces different types of ERP, presents a mathematical model of ERP generation, details the P300 potential (object of study of this work) and its usual elicitation protocol (oddball paradigm) for BCI (speller) construction.

2.2.1 Different Types of ERP

EEG is capable of recording a vast number of different neurological potentials. Among them, event-related potentials (ERP) are relevant both for diagnosis (DAVIES; GAVIN, 2007) and understanding cognitive processes (SALILLAS; YAGOUBI; SEMENZA, 2008). ERP are electric signals measured by EEG as a direct result of sensory, cognitive or motor events. As exemplified by Blackwood (1990), the hearing of specific tones, viewing of certain image patterns, reading of words and/or pressing of buttons can all elicit different ERP.

Arising as a physiological response to stimulation, these potentials are characterized by presenting a consistent waveform. Such waveform does not change drastically over time, remaining almost the same whenever a new stimulus occurs (SUR; SINHA, 2009).

ERP are commonly divided into two categories. When a specific event-related potential presents peaks within the first 100 ms post-stimulus, it is called an exogenous, or sensory ERP, and is strongly dependent on the physical characteristics of the stimulus. However, when the ERP is best characterized by a peak that occurs after 100 ms post-stimulus, it usually involves processing by associative cortical areas and therefore possesses higher variability, being called endogenous or cognitive ERP (SUR; SINHA, 2009).

When recorded by means of EEG, the amplitudes of ERP range from 1 to 10 μV. This is at least ten times lower than typical EEG amplitudes, that is, ERP waveform is masked by background brain activity (NIEDERMEYER; SILVA, 2004). For this reason, ERP detection is an object of intense research (HUGGINS *et al.*, 1999; BOSTANOV; KOTCHOUBEY, 2006; CECOTTI, 2015).

A typical ERP waveform is composed by several peaks and valleys, respectively named by the letters "P" or "N" to indicate a positive or negative voltage deflection.

Moreover, since the latency of peaks and valleys occurrence is essential for potential characterization, its value in milliseconds is usually added besides P or N (LUCK, 2005). For example, P100 identifies a positive voltage deflection occurring approximately 100 ms post-stimulus.

Figure 2.3 exemplifies a typical ERP waveform, composed by many enumerated components. It is worth noting the inversion of the vertical axis, a common practice in the representation of event-related potentials that has its origins in the clinical literature.

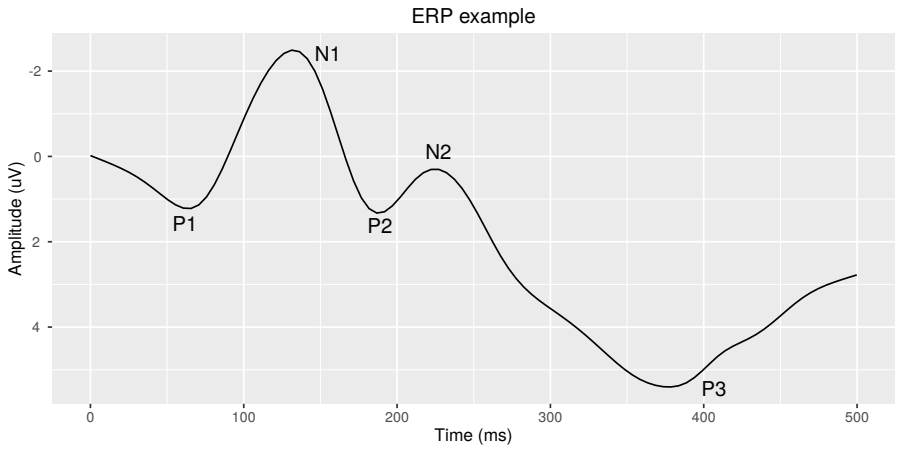

Figure 2.3 – Illustration of generic ERP waveform.

In a detailed study, Sur e Sinha (2009) cite the following typically encountered ERP:

- **P50:** is the greatest peak between 40 and 75 ms post-stimulus, whose amplitude is calculated as the difference between the greater peak occurring inside this interval and the greater valley that occurs before it. When an individual directs his attention to stimuli of interest, ignoring background stimuli, this potential appears, being related to conditions that require selective attention. The P50 is usually elicited by paradigms that involve repetitive clicks or steady state tones, usually via the auditory pathway;
- **N100/N1:** is the largest valley inside the interval between 90 and 200 ms post-stimulus, being elicited when a deviant stimulus occurs;
- **P200/P2:** is the largest peak inside the interval between 10 and 250 ms post-stimulus, arising in association with N100, composing the N1/P2 component;
- **N200/N2:** is the largest valley occurring after 200 post-stimulus, being elicited by any discernible change in a repetitive auditory stimulation;

- **N300:** a recently discovered ERP, it is elicited in the context of semantic consistency and expectation;
- **N400:** occurring between 300 and 600 ms post-stimulus, this valley is associated with semantic incongruity, which happens when one hears phrases that makes no sense;
- **P600:** this peak appears in the context of language processing, for example when a sentence has a syntax violation, has an unusual syntactic structure or has a complex syntactic structure;
- **MRCP:** movement-related cortical potentials are composed by a series of potentials that occur at instants close to movement-related activities. They can occur before, after or during the execution of movement and are associated with a cortical state of readiness for movement execution;
- **CNV:** the contingent negative variation was one of the first ERP discovered, and can be elicited by a standard protocol of motor response reaction time. An initial stimulus (S1) serves as a preparatory signal to an action stimulus (S2), to which the individual must respond. The CNV can appear at the beginning or the end of the interval between the two stimuli. When occurring at the beginning, it is indicative of excitatory processes, while when CNV occurs at the end of the interval it indicates attention to the task being performed;
- **PINV:** the post-imperative negative variation is the delay that occurs in the determination of CNV, indicating sustained cognitive activity;
- **P300:** the focus of this dissertation, this potential is characterized by a peak occurring nearly 300 ms post-stimulus and is the ERP on which most research has been performed until this date.

2.2.2 Event-Related Potential Models and Grand Average

A model for event-related potentials can be derived considering that the ERP waveform remains the same when successive presentations of a stimuli occur, and that the background brain activity (background EEG) can be modeled as zero-mean additive noise (NIEDERMEYER; SILVA, 2004).

From these premises, the ERP can be represented as an additive model, as illustrated in Figure 2.4, where $x[n]$ is the stimuli that elicits the ERP $s[n]$; $h[n]$ is the system transfer function, that corresponds to brain processes; $\nu[n]$ denotes the background EEG; $y[n]$ is the measured signal (NIEDERMEYER; SILVA, 2004; MELGES, 2009).

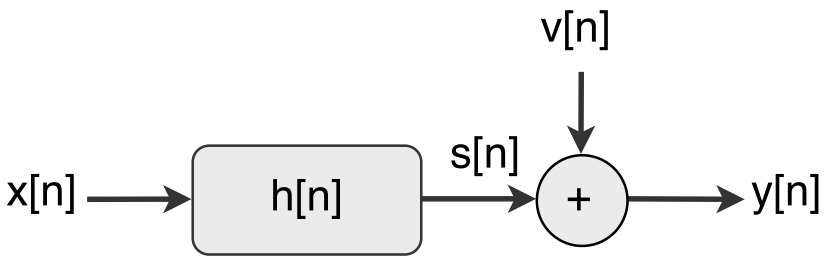

Figure 2.4 – ERP model. Adapted from (MELGES, 2009).

From the ERP model derived, the i-th epoch of the measured signal can be represented by (NIEDERMEYER; SILVA, 2004):

$$y_i[n] = s[n] + \nu_i[n] \tag{2.1}$$

Since $s[n]$ is the same in all epochs, the i index was omitted. Since spontaneous EEG has amplitudes that are many times higher than the ERP's, the application of methods capable of enhancing the potential's signal-to-noise ratio (SNR) is required. In this context, one of the simplest and most often employed techniques to this purpose is the grand average, a procedure that performs the mean of many EEG epochs, synchronized at the instant of stimulation.

From Equation 2.1, grand average calculation leads to:

$$\hat{s}[n] = \frac{1}{M}\sum_{i=1}^{M} y_i[n] = \frac{1}{M}\sum_{i=1}^{M} s[n] + \frac{1}{M}\sum_{i=1}^{M} \nu_i[n], \tag{2.2}$$

where $\hat{s}[n]$ is an estimator to the stimuli response; M is the number of EEG epochs used in the calculation. Since $\nu[n]$ has zero mean, the second summation will tend to zero as M increases, approximating the estimator $\hat{s}[n]$ of the actual ERP.

2.2.3 The P300 Potential

The P300 potential is an ERP component found by Sutton *et al.* (1965) and, since its discovery, has been one of the most studied by researches, mainly in two contexts: i) development of brain-computer interfaces; ii) detection of concealed information, especially by researches that aim to replace the polygraph.

The P300 is characterized by a positive peak ranging from 2 to 5μV, occurring between 300 and 600ms post-stimulus. It originates in the frontal and temporo-parietal regions of the scalp, with higher amplitude in the Fz, Cz and Pz derivations. Typically, the amplitude increases from the forehead to the parietal region (POLICH, 2007). Despite the fact that the maximum P300 amplitude occurs in the parietal region, the largest association of amplitude and latency is found on the frontal region (POLICH, 1997).

The latency of this potential is considered to be inversely proportional to the speed of stimulus classification by the brain. Therefore, shorter latencies indicate a higher mental classification performance, when compared to greater latencies. The amplitude level of P300 indicates the subject's attention to the stimuli and is directly proportional to the subjects' level of awareness (SUR; SINHA, 2009).

The elicitation of this ERP occurs when a person focuses its attention on a symbol of interest (a *target* event) that is presented infrequently and interchangeably with other insignificant symbols, but with higher stimulation frequencies(a *non-target* event) (ROSENFELD, 2011).

P300 occurs by means of active and passive processes. The active process occurs when the subject pays voluntary attention to the stimuli, while the passive process occurs involuntarily, together with other perceptual properties of the brain (COMERCHERO; POLICH, 1999).

Depending on whether the elicitation of the potential occurs by means of active or passive processes, P300 suffers variations on its amplitude and latency. Hence, it is commonly divided into two subcomponents: the passive component is called P3a; the active component, generated for active processes of the brain and highly dependent on the attention, is called P3b (POLICH, 2007). When P300 is used in brain-computer interfaces, the P3b subcomponent is preponderant.

As is the case with all event-related potentials, the signal-to-noise ratio of P300 is very low. Then, the grand average of a high number of EEG epochs is required to allow visualize the potential's waveform. Figure 2.5 exemplifies the P300's waveform for *target* (solid line) and *non-target* (dashed line) events.

2.2.4 P300 Speller

To elicitate the P300, an experimental protocol commonly known as row-column paradigm (RCP) is employed. This protocol uses an array of symbols (or letters) that are grouped into rows and columns, and that is the reason behind its name (FARWELL; DONCHIN, 1988).

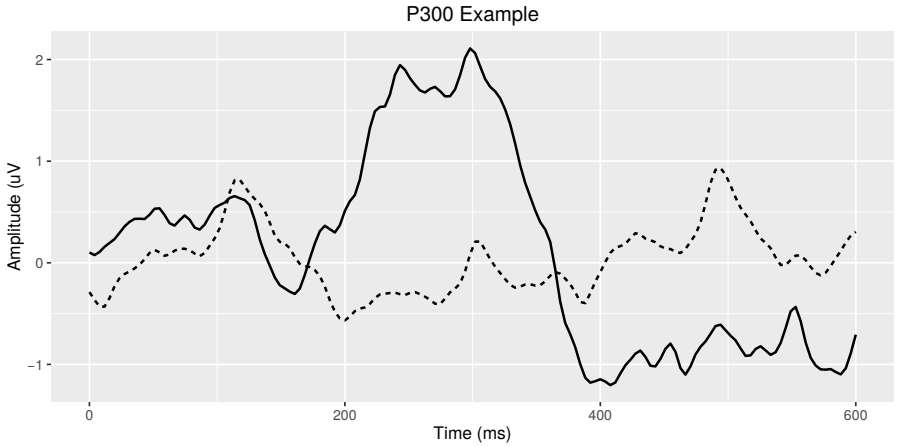

Figure 2.5 – P300 waveform example. The solid line contains a *target* event; the dashed line contains a *non-target* event.

In this protocol, the subjects are instructed to fix their gaze into the symbols of a given pre-defined sequence (word), focusing their attention at one symbol at a time. The array used in the protocol is illustrated in Figure 2.6.

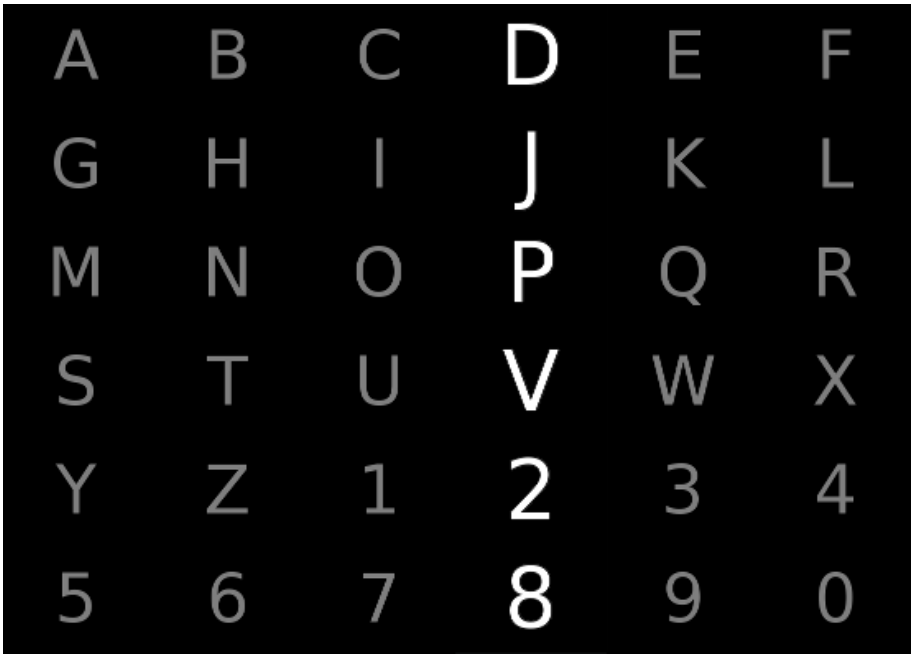

Figure 2.6 – Symbol's array commonly used to elicit P300.

Each row and each column, among 12 possible options, are intensified (for example, set to a more intense color) during an interval known as intensification interval. The period in which all rows and columns are kept in a neutral state is called non-intensification interval. The row or column to be intensified is defined randomly, which is required to elicit the P300 (FARWELL; DONCHIN, 1988).

A *trial* is defined as the period consisting of the intensification of all rows and columns once. Normally, there can be more than one trial for each symbol. The waiting time between *trials* is called inter-trial interval.

When the subject is submitted to the protocol, he/she is instructed to mentally count the number of times that the pre-selected symbol is intensified, so as to ensure that he (or she) pays attention to the stimuli being presented. The subjects are also instructed to avoid excessive blinking or moving their eyes in order to avoid artifacts.

When the row or column containing the pre-selected symbol is intensified, a *target* event occurs, possibly leading to P300's elicitation. The intensification of all other rows or columns that do not contain the pre-selected symbol will not lead to P300 elicitation and is called a *non-target* event.

In summary, in each *trial* there are two events of the type *target* (when a row or column containing the pre-selected symbol is intensified) and 10 events of the type *non-target* (all other intensifications).

It is expected that a *target* will elicit the P300 (PIRES; NUNES; CASTELO-BRANCO, 2011). Therefore, when identifying the P300's occurrence, it is possible to identify the row and column containing the symbol of interest.

3 P300 and Brain-Computer Interfaces

In this chapter, the application of P300 in brain-computer interfaces and the most recent works of the literature focusing on single-trial P300 detection are discussed.

3.1 Brain-computer Interfaces

Brain-computer interfaces are integrated hardware and software that allow users to control devices and environments, using brain signals as the source for performing actions (NICOLAS-ALONSO; GOMEZ-GIL, 2012). Therefore, BCI are capable not only of detecting specific brain activities or mental states, but also to translate these events into useful commands (WOLPAW *et al.*, 2002).

Wolpaw *et al.* (2002) cites the following methods commonly used to non-invasively monitor brain activity: positron emission tomography (PET), functional magnetic resonance imaging (fMRI), functional near-infrared spectroscopy (fNIRS), magnetoencephalography and EEG. However, when the focus of monitoring brain signals is to use them as the basis of BCI, EEG is the most used technique. As pointed out by Nicolas-Alonso e Gomez-Gil (2012), EEG offers good signal quality and, at the same time, is a low cost and easy to use technique. Moreover, EEG presents high temporal resolution, what is essential to obtain high information transfer rates (ITR) – a parameter widely employed to evaluate BCI performance.

There are two principal BCI classes: dependent and independent. Dependent BCIs are those that require adequate behaviour of certain functions (motor function, for example) to operate adequately, such as BCI based on visual evoked potentials (VEP). Such ICM depends on the integrity of the extra-ocular muscles for gaze direction (ELSHOUT; MOLINA, 2009). On the other hand, the independent BCI, such as those based on the P300, depends more strongly on the attention of the user than on the precise orientation of the eyes (FABIANI *et al.*, 1987). Independent BCIs may be more useful for people with severe neuromuscular disorders, since they do not require the perfect functioning of the peripheral nerves and muscles (WOLPAW *et al.*, 2002).

There are three potential groups of BCI users: people who have lost all motor activity, such as individuals who suffer from amyotrophic lateral sclerosis; people who possess only residual movement, such as movement of the eyes or lips; and people who do not present motor deficit (NICOLAS-ALONSO; GOMEZ-GIL, 2012). Currently, people who fall into the first or second groups are the main candidates for continued use of BCI

because, although BCI still has much to improve, the severity of the disorders presented by these people makes BCI a feasible alternative (NICOLAS-ALONSO; GOMEZ-GIL, 2012).

However, most of the BCI developed to date are focused on training or demonstration. Despite the recent advances, the development of BCI faces great challenges that must be overcome to make use of such technology widespread (MOORE, 2003):

- To increase BCI information transfer rates, promoting improved interaction with the environment and other devices;
- To reduce classification error rates, which frustrates the user and complicates the interactions;
- To promote greater autonomy for BCI users regarding electrodes placement and configuration of electronic devices, that nowadays are performed by other people;
- To create methods that enable automatic connection of BCI;
- To reduce the cognitive load required for BCI operation, in order to make such devices user-friendly even outside of the laboratory environment.

In fact, many applications have showed that BCI can improve the life quality of the disabled population and their relatives (NICOLAS-ALONSO; GOMEZ-GIL, 2012). However, the existing challenges make the development of a BCI a complex task (WOLPAW *et al.*, 2002).

A general BCI architecture contains the components illustrated in Figure 3.1. Firstly, the neural states of the user are converted to electrical signals using electrodes placed on the scalp surface, recording neural signatures by means of EEG. The signals coming from electrodes are directed to an *amplification stage* that adequates the voltage to the level expected by the next stages (MASON; BIRCH, 2003).

After the *amplification stage*, the electrical signals pass through an artifact removal step, where artifacts are reduced or completely eliminated from the original signals. Analogic or digital filters, as well as other digital signal processing techniques, are commonly used at this stage (NIEDERMEYER; SILVA, 2004).

The *feature engineering stage* transforms collected signals into parameters that will be the basis for control of the BCI. A signal frequency spectrum is an example of

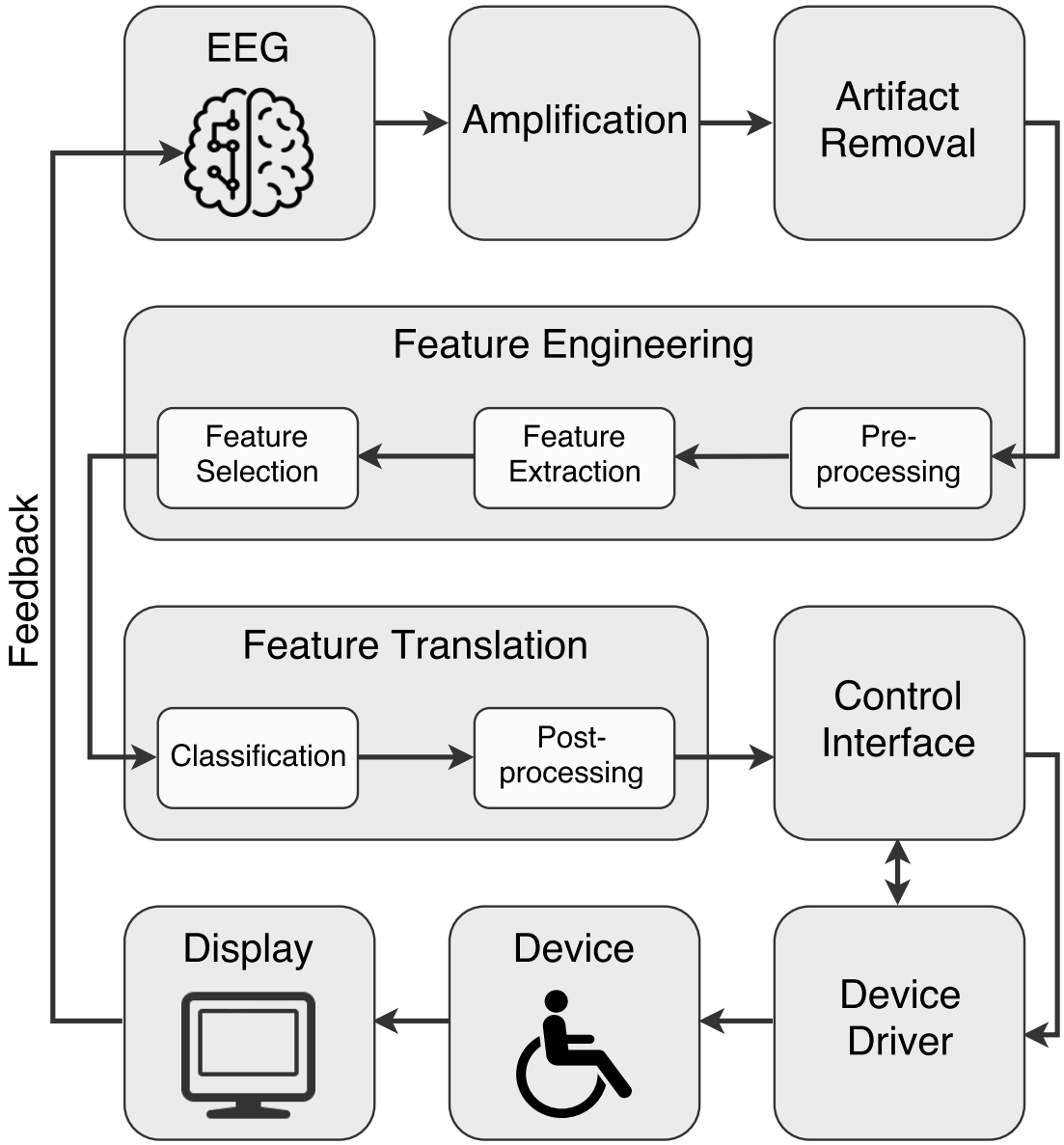

Figure 3.1 – BCI architecture.

generated feature, where the spectral power from alpha and beta bands can be identified and used for task control (MCFARLAND *et al.*, 2000).

This stage can be divided into three steps. The first is pre-processing, in which techniques that aim to enhance the SNR of the original signal are employed. Following this, the feature extraction step pulls out relevant parameters from the signal. Then, the number of parameters is reduced to eliminate redundancy and to reduce computational

efforts (decreasing dimensionality) (BASHASHATI *et al.*, 2007).

The characteristics generated in the previous step are then used as inputs of the *feature translator stage*. This stage can use linear or non-linear techniques, being subdivided into other two steps, classification and post-processing. In the *classification* step, the techniques employed transform the characteristics extracted from the neural states into logic signals. Finally, the *post-processing* step can be used to reduce classification errors or to increase the communication rate of the BCI (BASHASHATI *et al.*, 2007).

The generated logic signals are sent to a *control interface*, which converts them into specific commands for each BCI application. Controlling a motorized wheelchair or prosthesis and selecting specific actions in a computer program are examples of such applications. Afterwards, the commands are sent to the *device*, which can be designed for each application, or be a generic hardware and software platform, such as a microprocessor (MASON; BIRCH, 2003).

The *controlled device* is the last component of the BCI structure and covers a wide variety of apparatus and applications. Examples include neural prostheses, computers, speech synthesizers, televisions, lights and others (WOLPAW *et al.*, 2002).

3.2 P300-based BCI and its Applications

P300-based BCI uses different stimulation types to obtain ERP elicitation, including visual, auditory, and tactile stimuli. Whilst auditory stimuli use tonal frequency variations (FURDEA *et al.*, 2009; W; DONCHIN, 2006), tactile stimuli are generated by means of a belt that creates vibrations with different intensity levels (BROUWER; ERP, 2010).

However, the vast majority of P300-based BCI employ visual stimulation protocols, with the oddball paradigm being the most widely used. In such paradigm, the user is instructed to focus its attention when the symbols of interest are presented, which is usually accomplished by counting the number of times that a pre-defined symbol appears in a screen.

The P300 speller commonly uses this kind of protocol and consists of an alphanumeric character array where rows and columns are intensified one at a time, in a random order, such as the one shown in Figure 2.6 (FARWELL; DONCHIN, 1988).

If the user focuses its attention on the intensified row or column that contains the symbol of interest, the P300 is expected to be elicited. On the other hand, if a non-

interest symbol is presented, the potential will not be generated. As we mentioned earlier, when a symbol elicitates the P300, a *target* event is generated, while a *non-target* event is generated by the presentation of a non-interest symbol.

By detecting *target* and *non-target* events and, consequently, the respective rows and columns that elicitated the ERP, the P300 speller allows users to send a sequence of letters to the computer, effectively being a "virtual keyboard" controlled by means of the brain activity.

A modification of the P300 speller uses complete phrases instead of letters to increase information transfer rates. Hence, context-aware sentences, such as "Turn off the light", "I'm in pain", "I need to use the bathroom", "I'm hungry" are randomly intensified, allowing the user to inform what is his greatest need at the moment (W; DONCHIN, 2006).

A study was carried out about how many people could spell a five letter word with only 5 minutes of training, aiming to test the simplicity of using P300-based BCIs. 72.8% of the volunteers spelled words without making mistakes (GUGER *et al.*, 2009), which is better than motor-imagery based BCIs, where only 6.2% of the volunteers were able to successfully complete the proposed task, without training (GUGER *et al.*, 2003).

One of the great advantages of P300-based BCI is that they require minimal training in order to obtain high successful classification percentages. Since this was well-known, a considerable number of applications have been developed, besides the P300 speller (BAYLISS; BALLARD, 1999; BAYLISS, 2003; KÜBLER *et al.*, 2008; MUGLER *et al.*, 2010; ALOISE *et al.*, 2011). These applications vary from assistive technology that focus on improving life quality of motor-impaired people to applications that aim to widen BCI applicability to daily tasks and general public.

One of these applications, a BCI-controlled web browser, was developed and tested by healthy and ALS-diagnosed volunteers. A matrix in which each cell contained a *link* was employed, making internet navigation possible(MUGLER *et al.*, 2010). Healthy and ALS users obtained classification rates of 90% and 73%, and information transfer rates of $14.4 bits/min$ and $8.8 bits/min$, respectively. In addition, ALS-diagnosed volunteers reported great satisfaction in using this BCI (MUGLER *et al.*, 2010).

Another example is Brain Painting, which is a BCI-based painting application. In such BCI, a 8x6 matrix is presented, with each cell containing graphical information such as color and size of the line (KÜBLER *et al.*, 2008; MÜNSSINGER *et al.*, 2010). In this study, users were able to reproduce (copy) reference (example) paintings, showing the

potentiality of BCI even for leisure (KÜBLER *et al.*, 2008).

With the same objective of making people have fun, MindGame was designed to enhance standard electronic game controls, such keyboards, mouses and joysticks, with brain commands (FINKE; LENHARDT; RITTER, 2009). When the P300 potential is detected, it triggers the movement of an avatar placed on a three-dimensional map. Classification rates of up to 65% were achieved, using only one EEG epoch (single-trial detection). The user gradually receives evaluations of its performance as a mechanism of *neurofeedback*, in order to improve its performance.

In the domotics field, studies focused on the control virtual houses, including equipment such as television, radio, lamps and other items, have been developed. These works point out to a promising future for patients with neurological disorders, regarding home automation applications (BAYLISS; BALLARD, 1999; BAYLISS, 2003; ALOISE *et al.*, 2011).

P300-based BCI that allow subjects to control motorized wheelchairs are of great importance, as they can provide freedom of movement for the impaired population (REBSAMEN *et al.*, 2007). In this type of BCI, the symbols of interest are destination choices for the user, such as bathroom or kitchen. By focusing his/her attention on these symbols, P300 is elicitated, allowing users to move the wheelchair and reach the chosen destination (ITURRATE *et al.*, 2009). Reliability is the great challenge faced by this type of BCI, since locomotion in uncontrolled environments is more difficult due to the traffic of people and other factors. However, they represent an important gain in autonomy for patients.

As nowadays a large part of a person's daily actions involves the use of computers, a BCI that provides control of such specific device was developed, using a P300 speller embedded in the computer. However, the evaluation of this BCI showed that many efforts must to be employed to make such BCI useful in everyday life (ZICKLER *et al.*, 2011).

Regardless of the application, increasing successful classification rates and information transfer rates, and decreasing detection time are the main challenges faced when developing P300-based BCI. One of the most promising approaches to reduce classification time is to use a smaller number of EEG epochs to detect P300. However, single-trial techniques still have much to improve.

3.3 Single-trial P300 Speller Detection

In the last years, a variety of studies have used different techniques to achieve single-trial P300 detection for speller development. This section makes a brief review of

the most prominent works found in the literature about this topic. The methods, casuistry and main results of such studies are summarized in Table 3.1:

Table 3.1 – Summary of works dealing with single-trial P300 detection in spellers

Paper	**Subjects**	**Accuracy (%)**	**Methods**
Lenhardt, Kaper e Ritter (2008)	12	65.5	EEG Time Samples; PCA; LDA
Finke, Lenhardt e Ritter (2009)	11	65.0	EEG Time Samples; PCA; FLDA
Li *et al.* (2009)	1	76.7	EEG Time Samples; ICA
Li *et al.* (2012)	5	84.8	D metrics; Threshold Detection
Haghighatpanah *et al.* (2013)	2	65.0	Discrete Wavelets; ICA; LDA
Morales *et al.* (2014)	10	61.2	Features extracted from P300 peak; SOM Neural Network
Vareka e Mautner (2015)	5	72.8	Windowed Means; LDA
Magee e Givigi (2015b)	3	76.4	EEG Time Samples; Genetic Algorithm; Neural Network
Wu *et al.* (2016)	2	70.0	EEG Time Samples; Least-Angle Regression; Sparse LDA

Lenhardt, Kaper e Ritter (2008) used Principal Component Analysis (PCA) to extract features from EEG time samples, acquired from 10 different derivations. Each epoch contained EEG segment from onset of stimulus presentation and with duration of $800ms$, filtered between 1 and 9Hz. The principal components obtained fed a LDA classifier. This approach was tested in 12 subjects, achieving an average accuracy of 65.5% for single-trial detection.

As cited in the previous section, MindGame was developed by Finke, Lenhardt e Ritter (2009) and achieved an average accuracy of 65.0%, for 11 subjects. A combination of EEG time samples, PCA and Fisher's Linear Discriminant Analysis (FLDA) was used to classify the incoming signals.

Independent component analysis (ICA) was used by Li *et al.* (2009) to identify components that are more indicative of P300 occurrence – those whose coefficients are

larger for *targets* than for *non-targets* events. For this purpose, a template target signal was generated by calculating the grand average of some epochs containing P300, and the three independent components with larger coefficients were set as standard independent components. Then, for each new epoch, new components were computed and the correlation with the standard components was calculated. A threshold detector was used to classify the epoch based on the correlation values, and an average accuracy of 76.7% was obtained. However, these methods were tested for only 1 subject.

Li *et al.* (2012) derived a D metrics for analyzing EEG time series. In this study, epochs were low-pass filtered with a cutoff frequency of 10 Hz and a small number of epochs was used to generate a target template. Then, for each new incoming signal, the variance-based metrics was calculated for all channels, thresholds were defined for these features and such thresholds used in the classification process. An average accuracy of 84.8% on 5 subjects was achieved in this work.

Discrete Wavelet Transforms were applied to decompose EEG epochs (duration of 600ms post-stimulus; band-filtering from 0.3 to 40Hz) into different levels of high frequency (details) and low frequency (approximations) components (HAGHIGHATPANAH *et al.*, 2013). Then, ICA was employed to decompose each wavelet component into its independent components (IC). The IC with higher coefficient values for *targets* than for *non-targets* were selected, and fed a LDA classifier. The described methods were applied to 2 subjects, achieving an average accuracy of 65%.

Morales *et al.* (2014) used EEG epochs low-pass filtered at 50Hz to estimate P300 waves, searching it between the two lower minima of each epoch. From P300 estimates, six features were extracted, such as the initial and end time of the lower peaks of the waveform and the P300 frequency, defined as the inverse of the time-lapse between such points. After, a SOM (Self Organized Map) neural network was trained to classify each trial from 10 subjects, and an average accuracy of 61.2% was obtained.

Vareka e Mautner (2015) employed the Window Means Paradigm to extract features from EEG epochs band-pass filtered between 0.1 and 8Hz. According with such paradigm, the interval between 200 and 500ms was divided into six smaller time intervals of 50ms each. The EEG samples contained in each of these intervals were averaged to generate the feature vector that fed a LDA classifier. This technique was tested with 5 subjects and obtained an average accuracy of 72.8%.

A neural network with 10 neurons in the input layer, 10 hidden neurons and two outputs was employed by Magee e Givigi (2015b) to classify trials based on features generated by a genetic algorithm. The chromosomes were composed of time features,

calculated from EEG epochs (band-filtered from 0.3 to 40 Hz) with duration of 780ms from the onset of stimulus presentation and filtered between 0.3 and 40Hz. These methods were validated on 3 subjects, achieving an average accuracy of 76.4%.

When trying to detect single-trial P300, sometimes the features space dimension is much higher than the number of observations, causing the within-class covariance matrix to not have full rank. With this problem in mind, Wu *et al.* (2016) used least-angle regression to select the best EEG time features and Sparse LDA to detect P300. This methodology was tested in 2 subjects and achieved an average accuracy of 70%.

Although many approaches have been used to detect single-trial P300 speller development, no method can be considered as golden standard. Also, different works use different datasets and different number of users, making the comparison of techniques for single- trial detection even harder.

4 Signal Processing Techniques

This chapter describes the signal processing techniques used in this dissertation, explaining each one of them in more detail.

4.1 Pre-processing

Pre-processing is the part of signal processing responsible for enhancing signal quality before other techniques are applied. Epoch rejection, signal filtering and common average referencing are described in this section as means of enhancing EEG signal quality.

4.1.1 Epoch Rejection

Epoch rejection methods are often used as preprocessing step in order to remove windows corrupted by high-amplitude artifacts. Such procedure ensures that most relevant data are processed, leading to better classification results (DELORME; MAKEIG; SEJNOWSKI, 2001).

One common criterion for epoch rejection is based on thresholds calculated from the statistical distributions of EEG signal amplitudes.

4.1.2 Signal Filtering

Another pre-processing step usually employed is signal filtering, which eliminates additive narrow-band (e.g.: network noise) noise and provides better signal-to-noise ratios. The most commonly used topologies are *Butterworth* and *Inverse Chebyshev* filters.

For P300 analysis, band-pass filters with low cutoff frequencies from 0.1 to $1Hz$ and high cutoff frequencies from 8 to $100Hz$ are used. Historically, a passband filter from 0.02 to $35Hz$ is often applied (FARWELL; DONCHIN, 1988).

However, recent studies have shown that the frequency band from 0.1 to $15Hz$ includes the most relevant content of the P300 spectrum (BOUGRAIN C. SAAVEDRA, 2012). Besides band-pass filters, *notch* filters are often employed to remove network frequency and harmonics (BOUGRAIN C. SAAVEDRA, 2012).

4.1.3 Common Average Referencing (CAR)

Usually, EEG signals are acquired using differential measurements, employing specialized instrumentation amplifiers (biosignal amplifiers). Therefore, a reference electrode

is necessary and choosing suitable location is essential to obtain high quality recording, especially for potentials with cognitive components, which can be evidenced or degraded by this choice. However, using only one electrode as reference can still lead to poor SNR for ERP such as P300, and re-referencing has been suggested to overcome this problem (ALHADDAD, 2012).

One of the re-referencing methods is called Common Average Referencing (CAR), which can enhance signal-to-noise ratios of EEG derivations by subtracting, from each one, the average of all recorded derivations:

$$CAR(V_i) = V_i - \frac{1}{N}\sum_{n=0}^{N} V_n, \tag{4.1}$$

where V_i is the derivation of interest; N is total number of recorded derivations; V_n is the n-th derivation on the scalp.

CAR is considered one of the best pre-processing techniques to highlight P300 potentials, providing excellent signal-to-noise ratios with simple calculations (ALHADDAD *et al.*, 2012).

4.2 Feature Generation

Target and non-target signals can be distinguished by characteristics in both time and frequency domains. This section describes metrics extracted/generated from EEG epochs to be employed as classification features to differentiate P300 and spontaneous EEG epochs.

4.2.1 Independent Component Analysis

Independent component analysis (ICA) is a technique that identifies the fundamental component sources of a given signal by finding a linear representation of nongaussian data so that the components are statistically independent (COMON, 1994).

The representation as independent components tries to capture the essential structure of the data, facilitating the tasks of feature extraction and signal separation (HYVARINEN; OJA, 2000).

ICA is used in a plethora of applications, including EEG signal analysis to separate the brain activity of interest (like P300) from spontaneous EEG. This approach is based

on the assumption that brain activity and P300 have distinct sources, leading to statistical independence (VIGáRIO *et al.*, 1997; LI, 2010).

Thus, let us consider that a given signal x_i (EEG derivation, in this study) can be expressed as a linear combination of j independent components (IC) $s_1...s_j$, such that (HYVARINEN; OJA, 2000):

$$x_i = a_{i1}s_1 + a_{i2}s_2 + \ ... \ + a_{ij}s_j, \tag{4.2}$$

where $a_{i1}...a_{ij}$ are unknown weights; x_i and $s_1...s_j$ are random variables with zero-mean. Zero-mean assumption can be achieved by removing the mean values of the original random variables, if necessary.

Equation 4.2 can be re-written in matrix form:

$$\mathbf{x} = \mathbf{A}\mathbf{s}, \tag{4.3}$$

where $\mathbf{x}$ is an i x n matrix; $\mathbf{A}$ is an i x j matrix; $\mathbf{s}$ is an j x n matrix (with n being the number of samples, omitted from equations for simplicity). Equivalently:

$$\mathbf{x_i} = \sum_{j=1}^{n} a_{ij}s_j \tag{4.4}$$

Hence, Equations 4.3 and 4.4 represent mathematically the independent component analysis model (HYVARINEN; OJA, 2000), which describes how data can be generated through a linear combination of independent components, allowing to identify which components are responsible for the signal (EEG) generation represented by the x_i derivations.

In Equation 4.3, only tvector $\mathbf{x}$ is known. Hence, the matrix $\mathbf{A}$ and the vector $\mathbf{s}$ need to be determined with the assumption that the components are statistically independent and their distributions are nongaussian (COMON, 1994). Thus, ICA separetes a signal into a linear combination of additive components. Assuming that the matrix $\mathbf{A}$ is square (HYVARINEN; OJA, 2000):

$$\mathbf{s} = \mathbf{W}\mathbf{x} \tag{4.5}$$

where $\mathbf{W}$ equals $\mathbf{A}^{-1}$.

Thus, ICA (Equation 4.4) will allow separating independent components $\mathbf{s}$ from the observation vector $\mathbf{x}$ and a mixture matrix $\mathbf{W}$. However, ICA generates two ambiguities.

The first one is that the variances (energies) of the independent components cannot be completely recovered. As both $\mathbf{A}$ and $\mathbf{s}$ are unknown, any scalar that multiplies one of the sources $\mathbf{s_i}$ can be cancelled by dividing the corresponding column of the matrix $\mathbf{A}$. Hence, the variance of each independent component is set to the unity. Moreover, the signals of the components cannot be recovered, but this is not important for most applications (HYVARINEN; OJA, 2000).

The second ambiguity is that the order of the ICs cannot be determined. Again, because both $\mathbf{A}$ and $\mathbf{s}$ are unknown, the order of the terms in Equation 4.4 can be freely rearranged, making impossible to determine the order of the ICs (HYVARINEN; OJA, 2000). Fortunately, neither of these ambiguities is important for our purposes.

The convergence of the ICA algorithm requires *non-Gaussianity* of the components. If the components are Gaussian and the mixing matrix is orthogonal, then two signals x_1 and x_2 are Gaussian with unit variance, as well as uncorrelated. The joint density will be (HYVARINEN; OJA, 2000):

$$p(x_1, x_2) = \frac{1}{2\pi} exp\left(-\frac{x_1^2 + x_2^2}{2}\right) \tag{4.6}$$

Therefore, the density is completely symmetric, making $\mathbf{A}$ impossible to be estimated. This is the reason why *non-Gaussianity* is the key to ICA estimation, which shall now be detailed (HYVARINEN; OJA, 2000).

Firstly, let us consider that the vector $\mathbf{x}$ is distributed accordingly to Equation 4.6 and that the ICs have identical distributions. ICA estimation can be carried out considering a linear combination of x_i:

$$y = \mathbf{w}^T\mathbf{x} \;=\; \sum_i \mathbf{w_i x_i}, \tag{4.7}$$

where $\mathbf{x}$ must be determined.

If $\mathbf{w}$ was one of the rows of $\mathbf{A}^T$, then the linear combination would be one of the independent components. So the question becomes how $\mathbf{w}$ can be determined such that it

equals one of these rows, which is the basic principle of ICA estimation. To explain this concept, let:

$$\mathbf{z} = \mathbf{A}^T\mathbf{w}, \tag{4.8}$$

leading to:

$$\mathbf{y} = \mathbf{w}^T\mathbf{x} \;=\; \mathbf{w}^T\mathbf{A}\mathbf{s} \;=\; \mathbf{z}^T\mathbf{s} \tag{4.9}$$

Now, $\mathbf{y}$ is a vector composed by linear combinations of the components of $\mathbf{s}$, weightened by $\mathbf{z}$. As even the sum of two independent variables is more Gaussian than any of the ICs, $\mathbf{z}^T\mathbf{s}$ is more Gaussian than any of the ICs, having the lowest level of Gaussianity when it is equal to one of the ICs. In this case, only one of the elements of $\mathbf{z}$ is nonzero.

Based on this principle, $\mathbf{w}$ can be estimated by finding a vector that maximizes the *non-Gaussianity* of $\mathbf{w}^T\mathbf{x}$, which would correspond to a $\mathbf{z}$ with only one nonzero component, meaning that $\mathbf{w}^T\mathbf{x} = \mathbf{z}^T\mathbf{s}$ equals one of the ICs.

Other than *non-Gaussianity*, ICA can also be estimated by minimization of mutual information and maximmum likelihood estimation. When estimating ICA by maximizing *non-Gaussianity*, kurtosis, negentropy and approximation of negentropy are used (HYVARINEN; OJA, 2000).

For a Gaussian random variable y, the Kurtosis is given by:

$$kurt(y) = E(y^4) - 3(E(y^2))^2, \tag{4.10}$$

where E is the expected value.

If a random variable y is Gaussian, then its fourth moment will be:

$$E(y^4) == 3(E(y^2))^2, \tag{4.11}$$

and so its Kurtosis will be zero.

Negentropy is based on the information theory concept of entropy, which quantifies the degree of information that an observation of a given variable will yield. Entropy of a discrete random variable Y is defined as (COVER; THOMAS *et al.*, 1991):

$$H(Y) = -\sum_i P(Y = a_i) log P(Y = a_i), \tag{4.12}$$

where a_i are all the possible values of Y.

In the case of a continuous variable $\mathbf{y}$ with density function $f(\mathbf{y})$, the generalization of entropy is called differential entropy and defined as (COVER; THOMAS *et al.*, 1991):

$$H(Y) = -\int f(\mathbf{y}) log f(\mathbf{y}) d\mathbf{y} \tag{4.13}$$

Accordingly to information theory, the more Gaussian a variable is, the largest entropy it will possess. Therefore, entropy can be used as a measure of *non-Gaussianity*. However, to obtain a measure that is always nonnegative and equal to zero when the variable is Gaussian, negentropy is used, given by (COVER; THOMAS *et al.*, 1991):

$$J(\mathbf{y}) = H(\mathbf{y}_{gauss}) - H(\mathbf{y}), \tag{4.14}$$

where $\mathbf{y}_{gauss}$ is a gaussian random variable with the same covariance matrix as $\mathbf{y}$.

However, while negentropy is one of the best methods to estimate *nongaussianity*, its calculation is very complex. Hence, approximations of negentropy are used.

One of such approximations is based on the maximum-entropy principle, which yields the following approximation:

$$J(\mathbf{y}) \approx \sum_{i=1}^{p} k_i [EG_i(y) - EG_i(\upsilon)]^2, \tag{4.15}$$

where k_i are positive coefficients; p is the number of coefficients used in the approxmation; υ is a Gaussian variable of zero mean and unit variance; G_i is a predefined nonquadratic function, such as:

$$G_1(u) = \frac{1}{a_1} log(cosh(a_1)u), \;\; G_2(u) = -exp(-u^2/2), \tag{4.16}$$

with $1 \leq a_i \leq 2$.

This negentropy approximation is used in the FastICA algorithm (HYVARINEN; OJA, 2000), used in this dissertation to perform ICA estimation.

4.2.2 Time and Frequency Extracted Parameters

Time and Frequency Extracted Parameters (TFE) is a technique that first generates a template for both signal classes (*target* and *non-target* events), using grand average.

The correlation between each incoming signal and its corresponding template is calculated:

$$\hat{r}_{xy}(k) = \sum_{m=-\infty}^{m=\infty} x^*[m]y[k+m], \tag{4.17}$$

where k is the number of time shifts applied and $*$ is the complex conjugate.

Moreover, both skewness and kurtosis is calculated for each incoming signal. The skewness of a random variable x is a measure of the asymmetry of the distribution, and is given by:

$$skew(x) = \frac{E[x^3] - 3\mu\sigma^2 - \mu^3}{\sigma^3}, \tag{4.18}$$

where $E(.)$ is the expected value; μ and σ are respectively the mean and the standard deviation of the distribution.

The kurtosis of a random variable x gives insights about the tail of the distribution, and can be calculated by:

$$kurt(x) = E(x^4) - 3(E(x^2))^2 \tag{4.19}$$

Regarding the frequency features, the power spectrum values correspondent to the quantiles of 0.05, 0.25, 0.5, 0.75, 0.95 and the correspondent frequencies are extracted as features.

4.2.3 Variance-Based Metrics

The Variance-Based Metrics (VBM) feature generation process was published by Viana, Scalzo e Melges (2016), generates a statistic parameter based on the variance of each electrode in the scalp and is calculated on windowed EEG epochs (discarding 10% of the points at the beginning and at the end of each epoch). This technique is a multivariate extension of the method proposed by Li (2010).

Let us consider EEG signals acquired from a subject submitted to P300 protocol. An EEG epoch containing P300 can be defined as:

$$x_0 = x_t + \nu, \tag{4.20}$$

where x_0 is the recorded EEG signal, with variance σ_0^2; x_t is the *target* signal (P300) with variance σ_t^2; and ν is the background noise, considered to be random and stationary with variance σ_ν^2.

Assuming that the *target* signal and the background noise are statistically independent, it follows that:

$$\sigma_0^2 = \sigma_t^2 + \sigma_\nu^2, \tag{4.21}$$

Now, suppose that the grand average of k *target* signals is calculated, being defined as x_{st}. Thus, the background noise variance will decrease to $\frac{\sigma_\nu^2}{k}$. Therefore, the grand average x_{st} can be described as:

$$x_{st} = \frac{1}{k}\sum_{i=1}^{k} x_{0i} \;=\; \frac{1}{k}\sum_{i=1}^{k}(x_{ti} + \nu_i), \tag{4.22}$$

where x_{0i} is the i-th recorded EEG epoch; x_{ti} is the i-th *target* epoch; and ν_i denotes the background noise present in the i-th EEG epoch.

Assuming that the variances of ν x_t remain constant with time, the variance of x_{st} can be written as:

$$\sigma_{st}^2 = \sigma_t^2 + \frac{\sigma_\nu^2}{k} \tag{4.23}$$

Hence, by increasing the number of epochs used, the variance of the grand average (P300 estimate) approaches the variance of the *target* signal. To this extent, two variable transformations can be made from x_0 e x_{st}:

$$T_1 = \frac{x_{st} + x_0}{2} \tag{4.24}$$

$$T_2 = \frac{x_{st} - x_0}{2} \tag{4.25}$$

If x_0 is a *target* signal, the variances of transformations T_1 and T_2, derived from Equation 4.24 and Equation 4.25, are given by:

$$var(T_1) = var(\frac{x_{st} + x_0}{2}) \ = \ \sigma_t^2 + \frac{(k+1)\sigma_\nu^2}{4k}, \tag{4.26}$$

$$var(T_2) = var(\frac{x_{st} - x_0}{2}) \ = \ \frac{(k+1)\sigma_\nu^2}{4k}, \tag{4.27}$$

A variance-based metrics, called D, can be calculated from $T1$ and $T2$ (LI, 2010). In the case x_0 is a *target* signal:

$$D = var(T_1) - var(T_2) \ = \ \sigma_t^2 \tag{4.28}$$

If x_0 is a *non-target*, then:

$$var(T_1) = var(T_2) \ = \ \sigma_t^2 + \frac{(k+1)\sigma_\nu^2}{4k} \tag{4.29}$$

Hence:

$$D = var(T_1) - var(T_2) \ = \ 0 \tag{4.30}$$

As Equation 4.28 and 4.30 show, this variance-based metrics can be used to perform P300 detection, since it presents a theoretical value that is equal to σ_t^2 for *target* and 0 for $non - target$ signals.

In order to improve separation between classes, VBM was calculated using a window that includes only samples of the signal from 10% of time-interval after stimulus and 10% before the end. This process eliminates possible P300 peaks elicitated in epochs adjacent to the epoch being analyzed, leading to better results.

The experimental values obtained for this metric are close to the analytically derived results. The probability density functions for *target* and *non-target* signals are shown in Figure 4.1. It can be seen that the variance-based metrics provides separation between the classes.

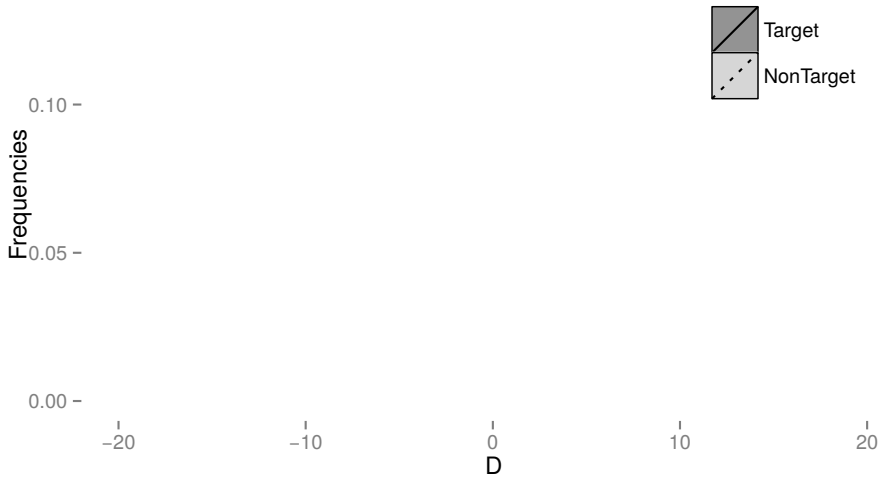

Figure 4.1 – Probability density function of D metrics for *target* and *non-target* signals.

4.2.4 Wavelet Coeficients

The Wavelet Transform (WT) exhibit some similarities with Fourier Transform since it can decompose a given function in a set of waves. However, WT performs decomposition into a set of functions called wavelets (WAV). While the latter projects signals into a space of sines and cosines – the frequency domain –, the former projects them into a space composed by functions that are localized both in time and frequency space. Hence, Wavelet Transforms can be used to perform time-frequency analysis of signals (CHUI, 2014).

In its most general form, the Continuous Wavelet Transform (CWT) can be described by (VALENS, 1999):

$$F_W(s,\tau) = \int_{-\infty}^{\infty} f(x)\psi^*_{s,\tau}(x)dx, \tag{4.31}$$

where F_W is the Wavelet Transform of the time-signal $f(t)$; ψ is an arbitrary function known as the mother Wavelet; s, τ are two new dimensions known as scaling and shifting, respectively; and * is the complex conjugate.

Wavelet transforms represent an infinite set of various transforms, that are generated by applying operations of shifting and scaling in the mother Wavelet $\psi_{s,\tau}$, defined as (VALENS, 1999):

$$\Psi(s,\tau) = \frac{1}{\sqrt{s}}\psi\left(\frac{t-\tau}{s}\right), \tag{4.32}$$

where ψ can be a set of base Wavelets defined according to the application and the term $\frac{1}{\sqrt{s}}$ is employed as an energy normalization factor across different scalings.

The mother Wavelets ψ need to obey two basic properties: admissibility and regularity. The admissibility can be expressed by the following equation (VALENS, 1999):

$$\int \frac{|\Psi(\omega)|^2}{|\omega|} dw < \infty, \tag{4.33}$$

where Ψ denotes the Fourier transform of ψ.

The admissibility property implies that, at zero frequencies, the Fourier transform of the mother Wavelet tends to zero:

$$|\Psi(\omega)|^2|_{\omega=0} = 0, \tag{4.34}$$

which also means that the average value of the mother Wavelet in the time domain must be 0:

$$\int \psi(x)dx = 0, \tag{4.35}$$

The regularity property states that a wavelet function must have some smoothness and concentration in the time and frequency domains, with a fast decay.

When dealing with continuous signals, such as EEG, one of the most used base functions is the Daubechie Wavelet, exemplified in Figure 4.2.

Figure 4.2 – Daubechie5 Wavelet example.

CWTs have some disadvantages such as redundancy and the need for an infinite number of wavelets to calculate the transform.

Trying to solve some of this problem, the Discrete Wavelet Transform (DWT) removes redundancy by applying scaling and shifting at discrete time-steps, rather than continuously. Therefore (DAUBECHIES *et al.*, 1992):

$$\Psi_{j,k}(x) = \frac{1}{\sqrt{s_0^j}} \psi \left(\frac{t - k\tau_0 s_0^j}{s_0^j} \right), \tag{4.36}$$

where j, k are integers; s_0 is a scaling step and t_0 is a shifting factor, that depends on s_0.

The DWT samples the time-frequency (scale) space in discrete intervals, determined by s_0. When $s_0 = 2$, one have the dyadic sampling, which is the most usual. It is also common to set $\tau_0 = 2$, ensuring dyadic sampling in the time domain.

Another step to remove redundancy in Wavelet transformation is to guarantee orthonormality, so that the discrete wavelets can be made orthogonal to their own dilations and translations by special choice of the mother wavelets (VALENS, 1999):

$$\int \psi_{j,k}(x) \psi^*_{m,n}(x) dx = \begin{cases} 1 \; if \; j = m \; and \; k = n \\ 0 \; otherwise \end{cases} \tag{4.37}$$

When DWT is employed on a continuous signal, a sequence of Wavelet coefficients (WAV) can be calculated in the process known as wavelet series decomposition, and can be used as features.

4.3 Classification

4.3.1 Linear Discriminant Analysis

Linear Discriminant Analysis (LDA) is a classifier that searches for a linear combination of features $\mathbf{x_i}$ that are capable of characterizing data classes. The combination of features that is found by LDA can then be used to classify new data samples, producing the output y (DUDA; HART; STORK, 2012).

The main assumption of LDA is that the conditional probability density functions of the classes are normally distributed, such that (VENABLES; RIPLEY, 2013):

$$p(\mathbf{x}|y) = 0, \quad (\mu_\mathbf{0}, \Sigma_0) \tag{4.38}$$

$$p(\mathbf{x}|y) = 1, \quad (\mu_\mathbf{1}, \Sigma_1), \tag{4.39}$$

where $\mathbf{x}$ is the feature vector; y is the output variable; $\mu_\mathbf{0}, \Sigma_0, \mu_\mathbf{1}, \Sigma_1$ are respectively the mean and covariance of classes $(0, 1)$.

With this assumption in mind, a classification criterion based on the Bayes optimum solution – which guarantees that classification error is due to noise present in the data – can be written as:

$$(\mathbf{x} - \mu_\mathbf{0})^T \Sigma_0^{-1} (\mathbf{x} - \mu_\mathbf{0}) + ln(\Sigma_0) - (\mathbf{x} - \mu_\mathbf{1})^T \Sigma_1^{-1} (\mathbf{x} - \mu_\mathbf{1}) + ln(\Sigma_1) > T, \tag{4.40}$$

where T is a previous defined threshold.

LDA assumes homoscedasticity, such that the covariances of both classes are identical and $\Sigma = \Sigma_0 = \Sigma_1$. With this assumption, the previous criterion is simplified to (VENABLES; RIPLEY, 2013):

$$\mathbf{w} \cdot \mathbf{x} > c, \tag{4.41}$$

where:

$$\mathbf{w} = \Sigma^{-1} (\mu_\mathbf{1} - \mu_\mathbf{0}) \tag{4.42}$$

$$c = \frac{1}{2}(T - \mu_{\mathbf{0}}{}^{T}\Sigma^{-1}\mu_{\mathbf{0}} + \mu_{\mathbf{1}}{}^{T}\Sigma^{-1}\mu_{\mathbf{1}}) \tag{4.43}$$

The means and covariances of the classes are not known, so they are obtained from a training sample. As the previous equations show, the class of a new sample can be found using only a linear combination of observed features.

LDA projects the features into a new space (linear discriminant space), using the vector $\mathbf{w}$. The class of a new sample x depends whether it is located on one side or another of a hyperplane perpendicular to $\mathbf{w}$ and whose location is defined by c (VENABLES; RIPLEY, 2013).

Figure 4.3 exemplifies this process.

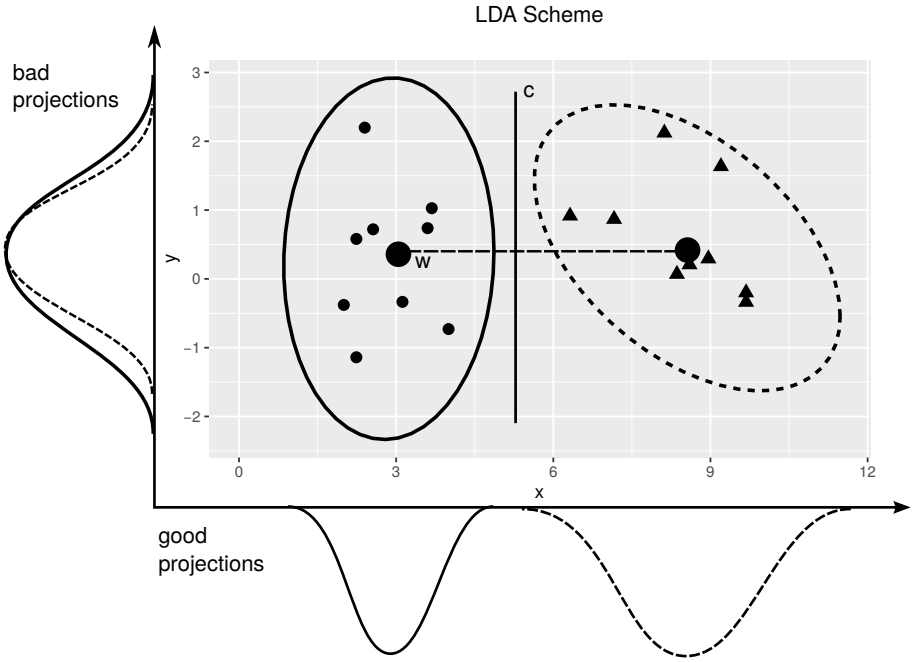

Figure 4.3 – LDA projection.

4.3.2 Logistic Models

Logistic Models (LOG) are statistical models used to predict the outcomes of categorical response variables given a set of input variables.

The relation between the features (input variables) and the dependent variable (output) is measured using a logistic function, which represents the cumulative logistic distribution (MYERS *et al.*, 2012):

$$E(y_i) = \frac{e^{(\beta_0 + x_i\beta_1)}}{(1 + e^{(\beta_0 + x_i\beta_1))}} = \frac{1}{(1 + e^{-(\beta_0 + x_i\beta_1))}}, \tag{4.44}$$

where $E(.)$ is the expected value of the response variable y_i; x_i is the i-th explanatory variable (feature); β_i is the coefficient associated with the i-th feature, and β_0 is the so called intercept.

This function is exemplified in Figure 4.4.

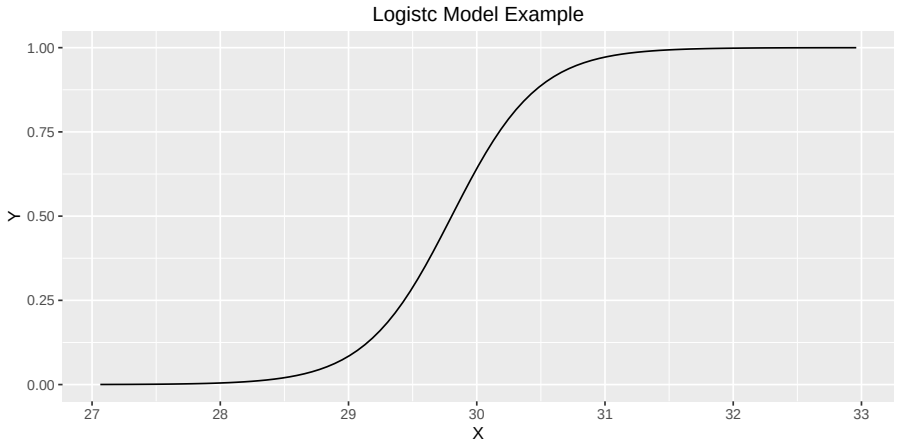

Figure 4.4 – Logistic function example.

When multiple features are allowed, Equation 4.44 is expanded to allow the modelling of the relation between y_i and the features x_{ik} from the coefficients β_k:

$$E(y_i) = \frac{1}{1 + e^{-(\beta_0 + \beta_1 x_{i1} + ... + \beta_k x_{ik})}} \tag{4.45}$$

The coefficients β_k are found using maximum likelihood estimation (MLE), which can find the best parameters θ of a model $f(x|\theta)$ given a set of observations $\mathbf{x}$.

The basic idea behind MLE is trying to estimate parameter values θ that maximize the likelihood that the observations $\mathbf{x}$ will be found again if one runs a new model fitted with the estimated parameters $f(\mathbf{x}|\theta)$ (MYERS *et al.*, 2012).

After the coefficients β_k are estimated with MLE, Equation 4.45 gives the expected value $E(y_i)$ as a probability outcome that can be used to predict the response variable value. If this value is compared to a threshold, then the logistic models can be used to classify incoming data (MYERS *et al.*, 2012).

4.3.3 Support Vector Machines

Support Vector Machines (SVM) are classifiers that find the best set of maximum-margin hyperplanes capable of correctly separating, and thus, classifying, a dataset. Optimum separation will occur when the distance between the set of hyperplanes and the nearest data samples is maximized (BOSER; GUYON; VAPNIK, 1992; CORTES; VAPNIK, 1995).

When doing binary categorization, a sample can be classified as belonging to one of two classes. In this case:

$$(x_{11},\ x_{12},\ ...,\ x_{1m}),\ ...\ (x_{n1},\ x_{n2},\ ...,\ x_{nm}) \in R^N \times (-1, 1), \tag{4.46}$$

where x_{nm} is the m-th sample from the input variable; N is the data dimension; $(-1, 1)$ are the labels of two arbitrary classes.

In SVM, the hyperplane that separates the new data $\mathbf{x}$ can be described by a weight vector $\mathbf{w}$ and by a *bias* term b. The class label of a new data sample can be inferred by:

$$f(\mathbf{x}) = \mathbf{w}.\mathbf{x} + b \tag{4.47}$$

In Equation 4.47, the data vector $\mathbf{x}$ was projected into the weight vector $\mathbf{w}$. If $\mathbf{w}$ is perpendicular to the hyperplane that separates the two classes, then the projection signal will define to which of the classes the input sample belongs.

To calculate $\mathbf{w}$, the samples that are located in the frontier between the two classes are used. For this reason, these samples are called *support vectors*, giving the name to the method (BURGES, 1998). A SVM illustration can be visualized in Figure 4.5.

The terms $\mathbf{w}$ and b should be chosen such that the distance between the parallel hyperplanes that separate data is maximized. These two hyperplanes are described by:

$$\mathbf{w}.\mathbf{x} - b = 1 \tag{4.48}$$

$$\mathbf{w}.\mathbf{x} - b = -1 \tag{4.49}$$

The distance between the two hyperplanes is given by $\frac{2}{||w||}$. Hence, for this distance to be maximized, it is necessary that $||\mathbf{w}||$ be minimized, at the same time that the points

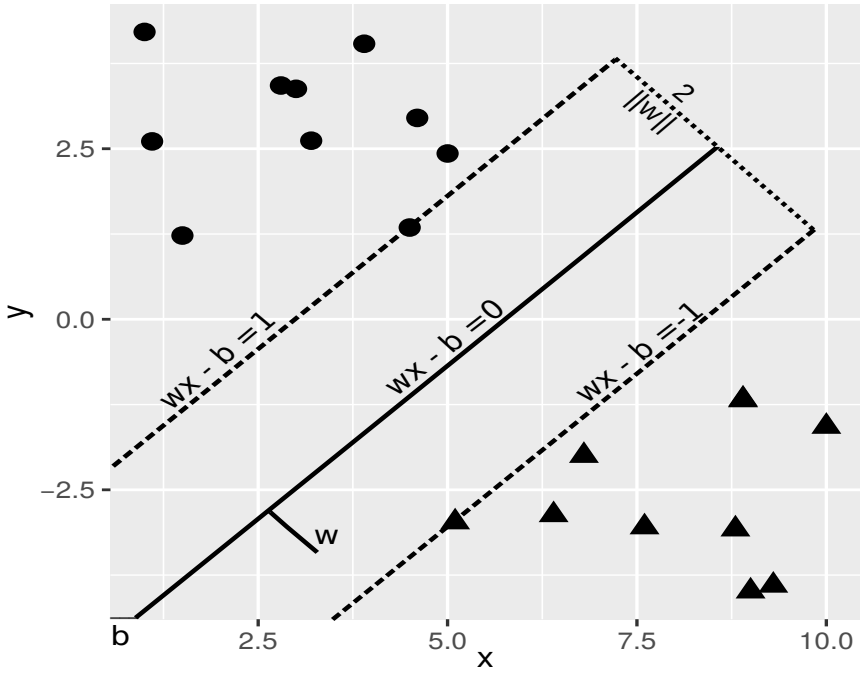

Figure 4.5 – SVM classifier scheme.

described by x must not lie inside the separation margin. The solution to this problem is given by:

$$w = \sum_{i=1}^{n} \alpha_i c_i x_i, \tag{4.50}$$

where α is a *Lagrange* multiplier associated with the problem constraints; c_i is the class label, such as $(-1, 1)$; and x_i is an input feature vector.

In order to allow a softer restriction to the classification margin in cases where data are not perfectly separable, the following equation is used (CORTES; VAPNIK, 1995):

$$\mathbf{w} = \sum_{i=1}^{N_s} \alpha_i c_i x_i, \tag{4.51}$$

where N_s is the number of support vectors used.

Therefore, replacing Equation 4.51 in Equation 4.47 yields:

$$f(\mathbf{x}) = \sum_{i=1}^{N_s} \alpha_i c_i (x_i.\mathbf{x}) + b \tag{4.52}$$

Usually, the inner product $(x_i.\mathbf{x})$ is replaced by a symmetrical *kernel* function $\phi(\mathbf{x}, x_i)$, turning the data space into a higher order feature space. Thus, more flexibility is obtained in order to better separate data (BURGES, 1998). One commonly used *kernel* function is the Gaussian one given by (KAPER *et al.*, 2004):

$$\phi(\mathbf{x}, x_i) = e^{\frac{||\mathbf{X}-x_i||^2}{2\sigma^2}}, \tag{4.53}$$

where σ is a chosen parameter.

Finally, if Equation 4.53 is replaced into Equation 4.52, it becomes:

$$f(\mathbf{x}) = \sum_{i=1}^{N_s} \alpha_i c_i \phi(\mathbf{x}, x_i) + b, \tag{4.54}$$

which is the equation that defines classification in SVM.

To solve this problem, the *Lagrange* multipliers can be found by optiming the following problem:

$$min_\alpha \; D(\alpha) = \frac{1}{2} \sum_{i,j} \alpha_i \alpha_j \phi(\mathbf{x_i}).\phi(\mathbf{x_j}) - \sum_i y_i.\alpha_i, \tag{4.55}$$

subject to:

$$\sum_i \alpha_i = 0 \tag{4.56}$$

$$0 \leq y_i \alpha_i \leq C, \tag{4.57}$$

where C is a tuning parameter of the algorithm.

Finally, by finding the optimal *Lagrange* multipliers and using Equation 4.54, the SVM algorithm can find the classes for each new feature vector.

5 Methodology

This chapter describes the P300 databases employed in this work, the signal processing steps, the performance evaluation metrics and the applied statistical analysis.

5.1 Databases

This section details the experimental protocol employed to build each one of the three P300 databases used to validate the techniques studied in this work.

5.1.1 Open Access P300 Speller Database

The Open Access P300 Speller Database (available in the link: <http://akimpech.izt.uam.mx/p300db/doku.php>) was made available by Ledesma-Ramirez *et al.* (2010) in order to facilitate P300 speller research and has been employed for benchmarking purposes, since it presents a larger casuistry if compared with other P300 studies.

The database contains data acquired from 24 healthy subjects, consisting of sixteen men and eight women, aged between 19 and 25 years old, without history of visual or neurological problems.

The subjects were submitted to the experimental protocol described in subsection 2.2.4. The intensification of rows and columns had a 62.5 ms duration, with a 125 ms interval between two consecutive stimuli (trials). Subjects waited for 2 seconds between consecutive runs.

Each subject performed 4380 trials, from which 730 trials corresponded to *target* events and 3650 trials to *non-target* events.

EEG signals were acquired using *gUSBAmp*, a sixteen channel biosignal amplifier. The right auricular lobe was used as reference and the ground was connected to the right mastoid. The signals were filtered between 0.1 and $60Hz$, and sampled at $256Hz$.

Signals were recorded from ten different electrodes: Fz, Cz, C3, C4, Pz, P3, P4, Oz, PO7, PO8 (part of 10-10 International System). The location of these electrodes can be seen in Figure 5.1.

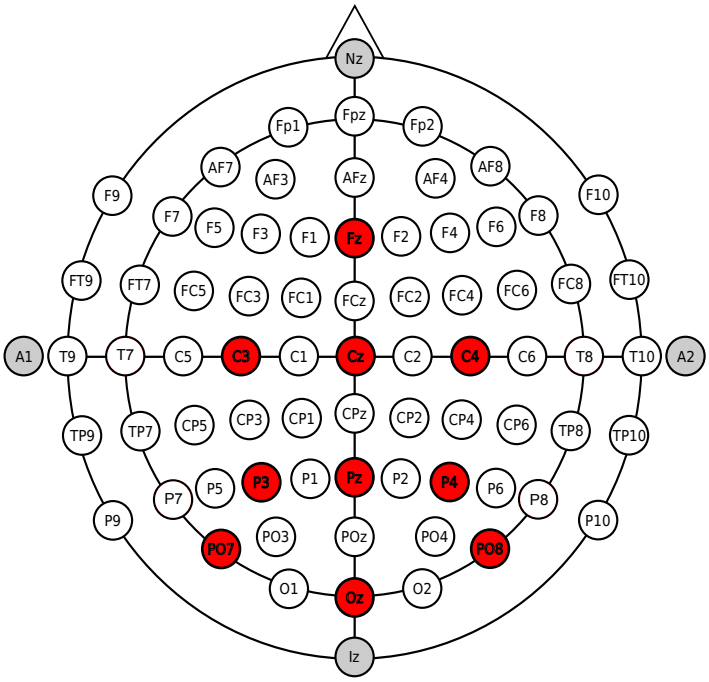

Figure 5.1 – Electrodes location for Open Access P300 Speller Database.

5.1.2 Guger Database

The Guger Database (available in the link: <http://bnci-horizon-2020.eu/database/data-sets>) was made available by Guger *et al.* (2009), and contains data acquired from 10 subjects that were submitted to the P300 Speller paradigm.

The experimental protocol described in subsection 2.2.4 was applied with the rows and columns intensified for an interval of 100 ms, with a 60 ms time lapse between two consecutive stimuli.

The protocol included 1800 trials, from which 300 trials corresponded to *target* events and 1500 trials to *non-target* events.

A *g.USBamp* biosignal amplifier was used to acquire EEGH signals. The ground electrode was located at the forehead and the reference was positioned on the right earlobe. The signals were sampled at $256Hz$, filtered between 0.5 and $30Hz$ and then downsampled to $64Hz$.

Eight derivations were recorded: Fz, Cz, Pz, P3, P4, Oz, PO7, PO8 (Figure 5.2):

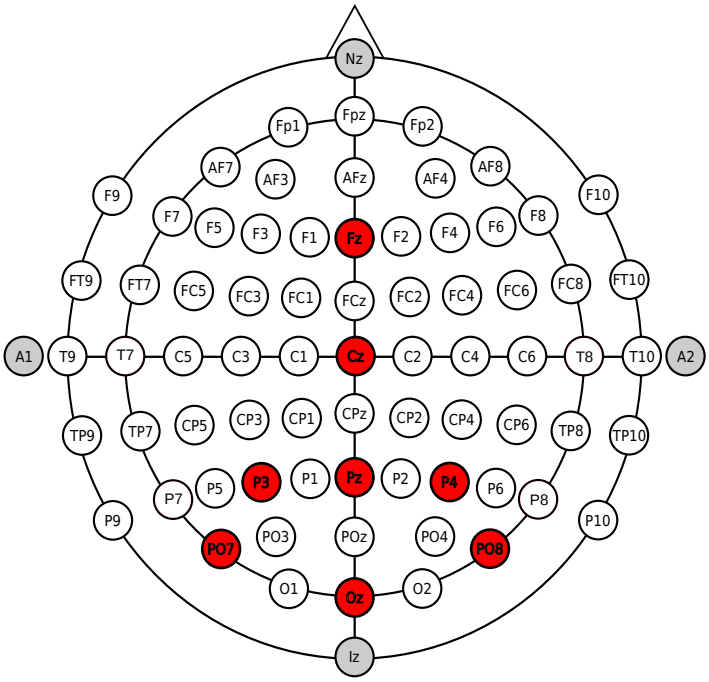

Figure 5.2 – Electrodes location for Guger Database.

5.1.3 ALS Database

The ALS Database (available in the link: <http://bnci-horizon-2020.eu/database/data-sets>) was made available by Riccio *et al.* (2013), and contains data recorded from subjects suffering from ALS disease submitted to the P300 Speller paradigm.

The database contains data acquired from 8 subjects, three women and five men, aged between 46 and 70 years old, with mean ALSFRS-R scores of 32 ± 8 (CEDARBAUM *et al.*, 1999).

For this experiment, the rows and columns were intensified for an interval of 125 ms, with a 250 ms lapse between two consecutive stimuli.

The experiment was composed of 4200 trials (700 *target* events and 3500 *non-target* events).

A *g.MOBILAB* biosignal amplifier was used to acquire EEG signals, with the right earlobe used as reference and the left mastoid as ground. The signals were sampled at $256Hz$ and filtered between 0.1 and $30Hz$.

Eight electrodes were used: Fz, Cz, Pz, P3, P4, Oz, PO7, PO8 (Figure 5.3):

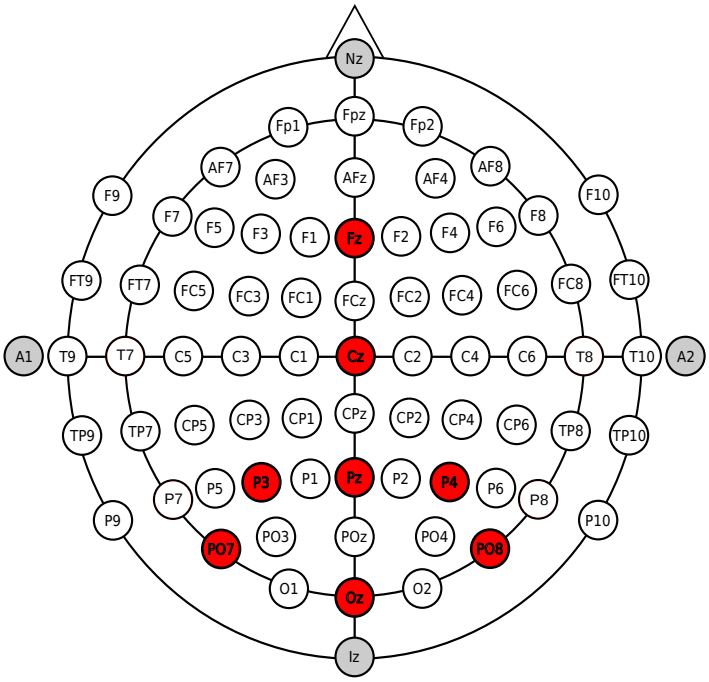

Figure 5.3 – Electrodes location for ALS Database.

5.2 Signal Processing Workflow

Signals were pre-processed by extracting 600ms-duration EEG epochs, stimuli-synchronized. The standard deviation σ_{ep} of raw EEG signals amplitudes was calculated and then used to decide whether epochs should be kept or rejected. Epochs consisting of more than 20% of samples higher than σ_{ep} or with more than 5% of consecutive samples higher than σ_{ep} were assumed to be noise-compromised and, hence, discarded.

The remaining epochs were band-pass filtered using a second order *Butterworth* notch filter between 59 and $61Hz$, cascaded with a second order *Butterworth* band-pass filters between 0.1 and $20Hz$. After filtering, the epochs were re-referenced using CAR, according to section 4.1.

After preprocessing, four different groups of features were generated using the signal processing techniques described in section 4.2: Independent Component Analysis, Time and Frequency Extracted Parameters, Variance-Based metrics and Wavelet Coefficients.

The generation of features requires the existence of a template for *target* and *non-target* signals. Therefore, for all techniques, 10% of the *target* trials were employed to generate the *target* template and 2% of the *non-target* trials were used to generate the *non-target* one. This is due to the fact that there are five times more *non-target* events

than *target* ones. The remaining epochs were used to generate features.

Regarding the TFE technique, the feature generation included time and frequency parameters (for both *target* and *non-target* trials), namely: skewness and kurtosis of the waveform of the incoming trial (IT); quantiles of power spectrum of the IT; correlation between IT and its corresponding template. All features were calculated individually for each EEG derivation. The feature vector was composed of 110 features for Open Access P300 Speller Database and 80 features for Guger and ALS databases.

For VBM technique, the feature vector was built by calculating D metrics for the incomings trials of each EEG derivation, using the equations described in subsection 4.2.3. The feature vector was composed of 10 features for Open Access P300 Speller Database and 8 features for Guger and ALS databases.

For WAV technique, the wavelets coefficients were calculated for boths the target and non-target templates, as explained in subsection 4.2.4. The coefficients that had higher absolute value for the *target* template than for the *non-target* one composed the feature vector. The feature vector was composed of 150 features for Open Access P300 Speller Database and 120 features for Guger and ALS databases.

Finally, for the ICA technique, the templates were used to extract independent components, seeking the ICs that best differentiate between both classes of signals. The extraction of ICs was performed 100 times, in order to get the better IC decomposition. The best ICs were considered those whose coefficients obtained from the *target* template achieved the highest difference from the coefficients extracted from the *non-target* template, saving the corresponding coefficients' matrix W, as described in subsection 4.2.1. Then, this matrix was used to extract independent components from the measured waveforms, for each incoming signal of the EEG derivations. The ICs were then decimated by a factor of 15 and concatenated as a feature vector. The feature vector was composed of 150 features for Open Access P300 Speller Database and 120 features for Guger and ALS databases.

After using ICA, TFE, VBM, and WAV for feature generation, three different classifiers were tested to detect the P300: linear discriminant analysis, logistic models and support vector machines.

A 5-fold validation procedure was used, randomly partitioning the generated features into five equal subsets. Four subsets were used as training data for the classifiers, and the remaining subset was used to validate the methods.

This was repeated five times (folds), using each of the five subsets once as validation

data. Then, the metrics obtained in the classifier for each fold were averaged to produce the final metrics estimation.

Finally, each classifier method was tested 100 times. The output values were averaged to obtain a mean performance for each method, which was then used for comparison. A schematic detailing the signal processing flow can be visualized in Figure 5.4

5.3 Performance Evaluation

To compare the performance of the different signal processing techniques and classifiers used in this work, four evaluation metrics were employed: Accuracy, AUC, Sensitivity and Specificity.

5.3.1 Accuracy

Accuracy (Acc) is one of the main metrics used to compare classification and detection methods, representing the percentage of samples that are correctly classified. Accuracy can be mathematically defined as:

$$Acc = \frac{T_P + T_N}{N}, \tag{5.1}$$

where T_P is the number of true positives (number of *targets* correctly identified); T_N is the number of true negatives (number of *non-targets* correctly identified); N is the total number of events.

5.3.2 Sensitivity

Sensitivity ($Sens$) is a measure of how many of the positive values found by a classifier are correct. For example, how much of the detected *target* events really contain P300. Therefore, it is defined as:

$$Sens = \frac{T_P}{T_P + F_N}, \tag{5.2}$$

where F_N is the number of false negatives (number of trials classified as *non-target* but that contain P300).

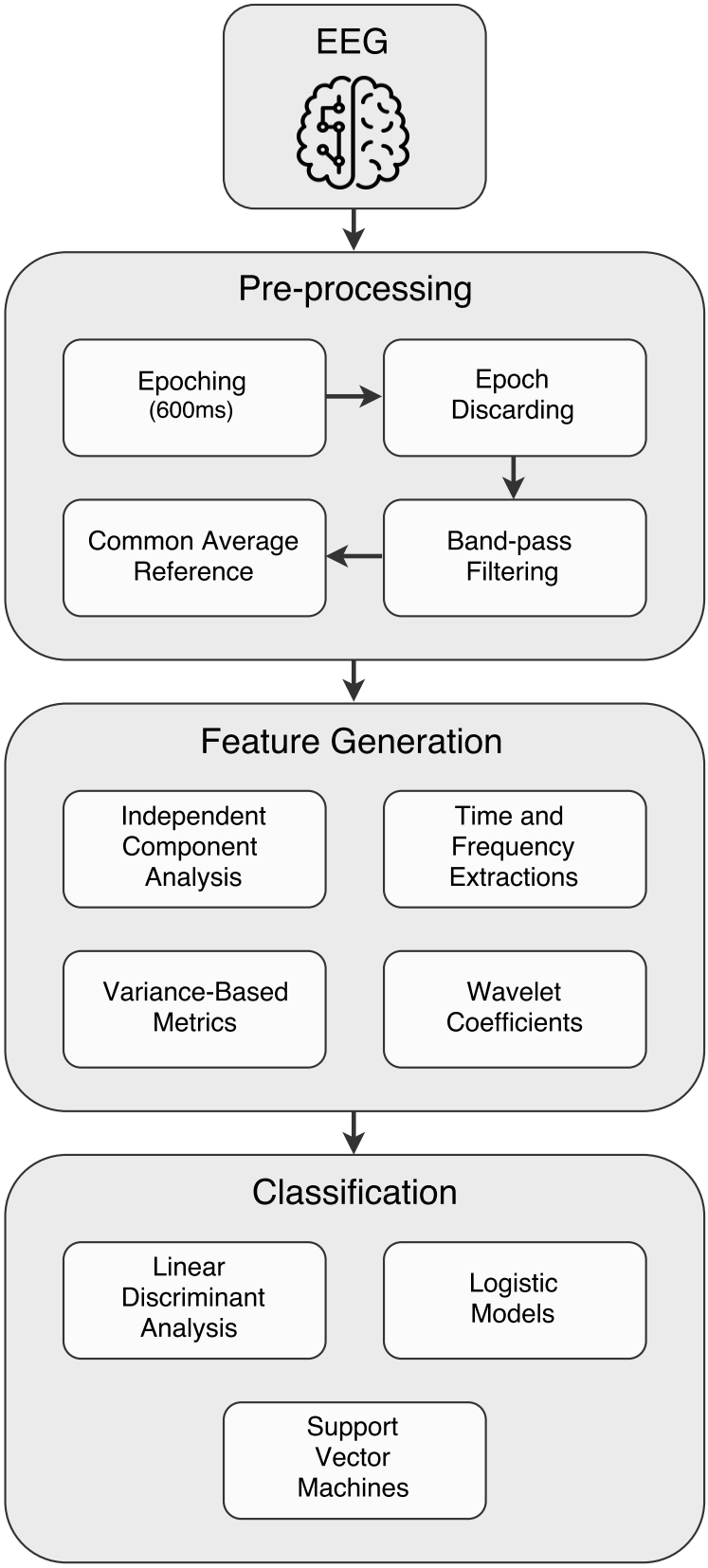

Figure 5.4 – Signal processing flow.

5.3.3 Specificity

Specificity (*Spec*) is a measure of the proportion between the number of true negatives identified and the total number of negatives (the number of *non-target* events identified that did not have P300). Specificity is calculated by:

$$Spec = \frac{T_N}{T_N + F_P}, \tag{5.3}$$

where F_P is the number of false positives (number of detected *target* events but that did not contain P300).

5.3.4 AUC

The Area Under the ROC Curve (*AUC*) is a metric commonly used to evaluate classifiers. When datasets are unbalanced, *AUC* can give better insights on the performance of classifiers than *Acc*, being an useful metric. *AUC* is defined as:

$$AUC = \int_{+\infty}^{-\infty} Sens(T)(1 - Spec(T))dT \tag{5.4}$$

where T is a probability threshold.

5.4 Statistical Analysis

In order to compare the performance of different techniques, the Friedman test was used. The Friedman test is a non-parametrical statistical test that can determine if the differences of performance obtained by different techniques are statistically significant (LEHMANN; ROMANO, 2006).

Because it is a non-parametric test, it doesn't need to assume any specific probability density function for the data being tested, which is useful when the data does not follow a particular distribution or when criteria for ANOVA application, such as homoscedascity, are not met.

Some requirements are needed for applying the Friedman test (LEHMANN; ROMANO, 2006): the evaluated metric should be ordinal or continuous, the datasets must be random samples taken from the population, datasets must correspond to observations from the same population on more than two occasions or conditions.

The null hypothesis for the test is that the distributions of the results of the techniques are the same across repeated measures, while rejection of the null hypothesis (alternative hypothesis) is that the distributions are different (LEHMANN; ROMANO, 2006).

In summary, Friedman's Test was applied to identify significant statistical differences in multiple treatments methods (feature extraction and classification method) given applied for on the same datasets (*target* and *non-target* trials on a P300 speller paradigm).

The Friedman test is particularly appropriate to test the performance of techniques, and can be used to compare Accuracy, AUC, Sensibility and Specificity (DEMŠAR, 2006). The same test was used to compare the best combinations of feature extraction technique and classifier.

A significance level of 0.05 was considered and the Bonferroni adjustment was made accordingly, using the Tukey test to perform post-hoc analysis (DEMŠAR, 2006).

6 Results

This chapter summarizes the results obtained with the application of the signal processing techniques and classifiers on the test databases.

6.1 Open Access P300 Speller Database

This section describes the results obtained when the methods were applied on the Open Access P300 Speller Database.

6.1.1 LDA Results

Table 6.1 summarizes the classification results obtained for each feature generation technique, using a LDA classifier. The median and inter-quartil range (IQR) for AUC, Sens. and Spec. are also shown. The best results were achieved using ICA, with a median accuracy of 83.4% and IQR of 8.3%.

Figure 6.1 shows boxplots that summarize the metrics for each features extraction technique, considering results of all subjects. The Friedman test indicated statistical differences with p-values of 0.006, 0.01, 0.02 and 0.04 for Acc., AUC, Sens. and Spec. respectively.

The post-hoc analysis is illustrated in Figure 6.2. For each performance metric, the boxplots representing the differences in performance between a set of two techniques are shown horizontally. When a significant difference is found in post-hoc analysis, the respective boxplot is marked in blue.

The analysis indicated that ICA performed better than TFE for Acc, AUC, Sens and Spec. No difference was found between all the other techniques, making all of them statistically comparable when a LDA classifier is used.

Table 6.1 – Summary of LDA results for Open Access P300 Speller Database

Technique		**Acc. (%)**	**AUC (%)**	**Sens. (%)**	**Spec. (%)**
ICA	Median	**83.4**	**83.4**	**82.8**	**84.6**
	IQR	**8.3**	**8.2**	**8.3**	**8.3**
TFE	Median	70.9	70.9	71.5	71.5
	IQR	13.5	13.4	13.5	13.5
VBM	Median	78.5	78.5	77.2	79.3
	IQR	8.4	8.5	8.4	8.4
WAV	Median	79.0	79.1	78.2	80.4
	IQR	5.6	5.6	5.5	5.5

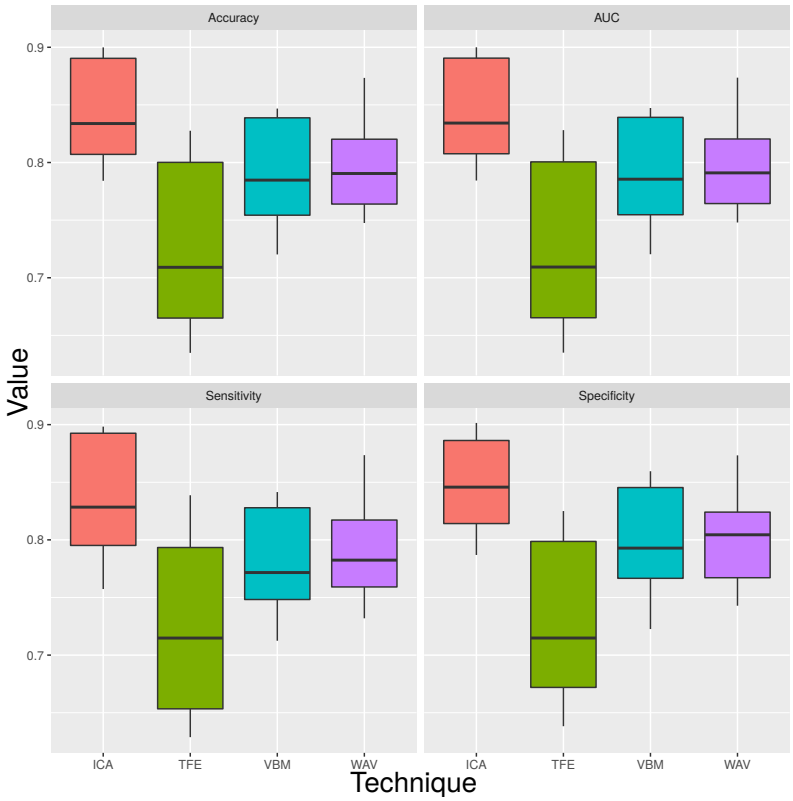

Figure 6.1 – LDA results for Open Access P300 Speller Database.

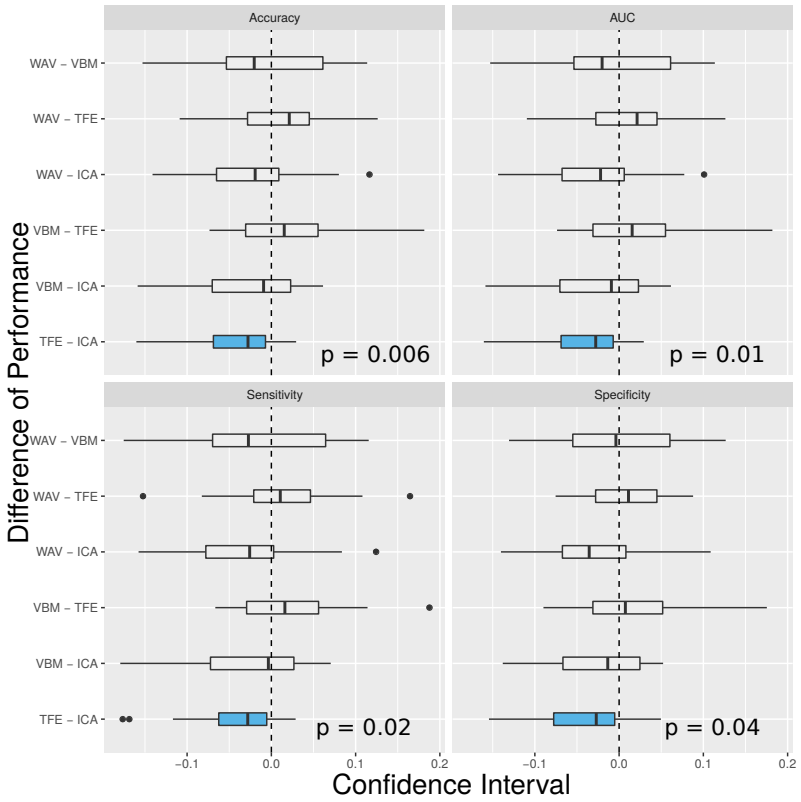

Figure 6.2 – LDA performance analysis for Open Access P300 Speller Database.

6.1.2 LOG Results

Table 6.2 summarizes the classification results (median and IQR for all metrics) obtained using a LOG classifier. Also for this classifier, the best results were achieved using ICA, with a median accuracy of 83.7% and IQR of 5.7%.

The boxplots summarizing for each metrics and each technique considering all subjects are shown in Figure 6.3. No statistical difference was found between the techniques, in terms of performance metrics.

Table 6.2 – Summary of LOG results for Open Access P300 Speller Database

Technique		**Acc. (%)**	**AUC (%)**	**Sens. (%)**	**Spec. (%)**
ICA	Median	**83.7**	**83.8**	**83.5**	**84.9**
	IQR	**5.7**	**5.8**	**5.9**	**4.4**
TFE	Median	72.2	72.2	71.6	73.8
	IQR	12.5	12.6	12.8	10.1
VBM	Median	77.9	78.0	77.6	80.7
	IQR	7.1	7.1	8.2	5.3
WAV	Median	81.8	81.8	81.7	82.4
	IQR	4.9	5.0	5.7	4.1

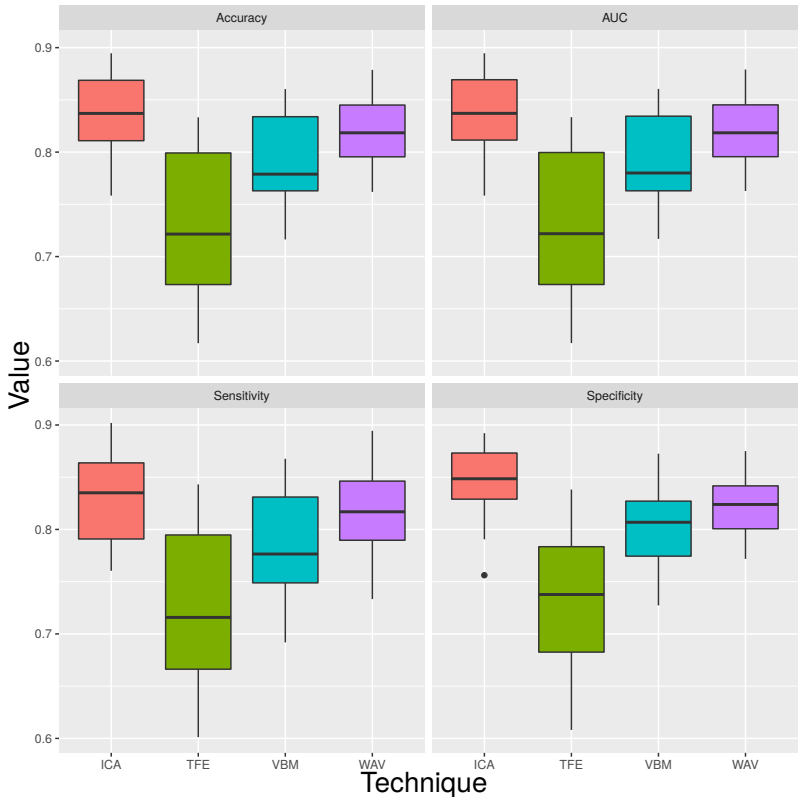

Figure 6.3 – LOG results for Open Access P300 Speller Database.

6.1.3 SVM Results

Table 6.3 summarizes the classification results obtained using a SVM classifier. The best results were achieved using ICA, with a median accuracy of 82.4% and IQR of 7.2%. Figure 6.4 shows boxplots that summarize the techniques results for all subjects. Statistical difference between techniques was found when the Friedman test was applied, resulting in p-values of 0.01, 0.02, 0.005 and 0.04 for Acc, AUC, Sens and Spec respectively.

Post-hoc analysis is illustrated in Figure 6.5, indicating that difference is due to better performance for ICA than for TFE, without statistical differences among ICA, WAV and VBM.

Table 6.3 – Summary of SVM results for Open Access P300 Speller Database

Technique		**Acc. (%)**	**AUC (%)**	**Sens. (%)**	**Spec. (%)**
ICA	Median	**82.4**	**82.4**	**82.2**	**83.9**
	IQR	**7.2**	**7.2**	**6.0**	**7.9**
TFE	Median	71.9	71.9	71.2	73.0
	IQR	14.0	13.9	12.9	11.8
VBM	Median	78.0	78.2	75.7	81.7
	IQR	7.6	7.4	8.2	5.6
WAV	Median	80.2	80.2	78.9	80.9
	IQR	5.5	5.5	5.7	5.9

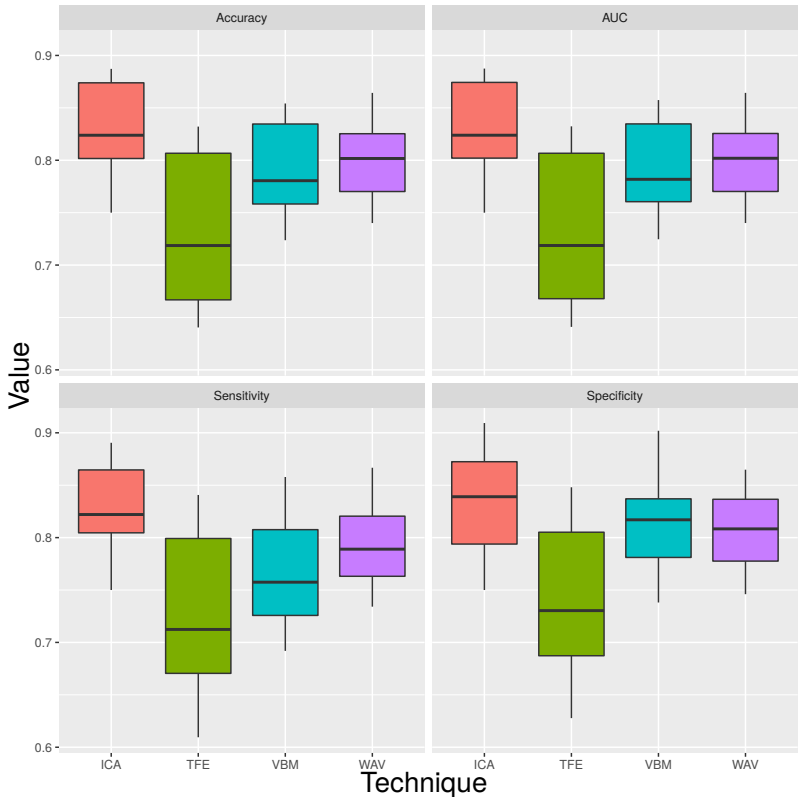

Figure 6.4 – SVM results for Open Access P300 Speller Database.

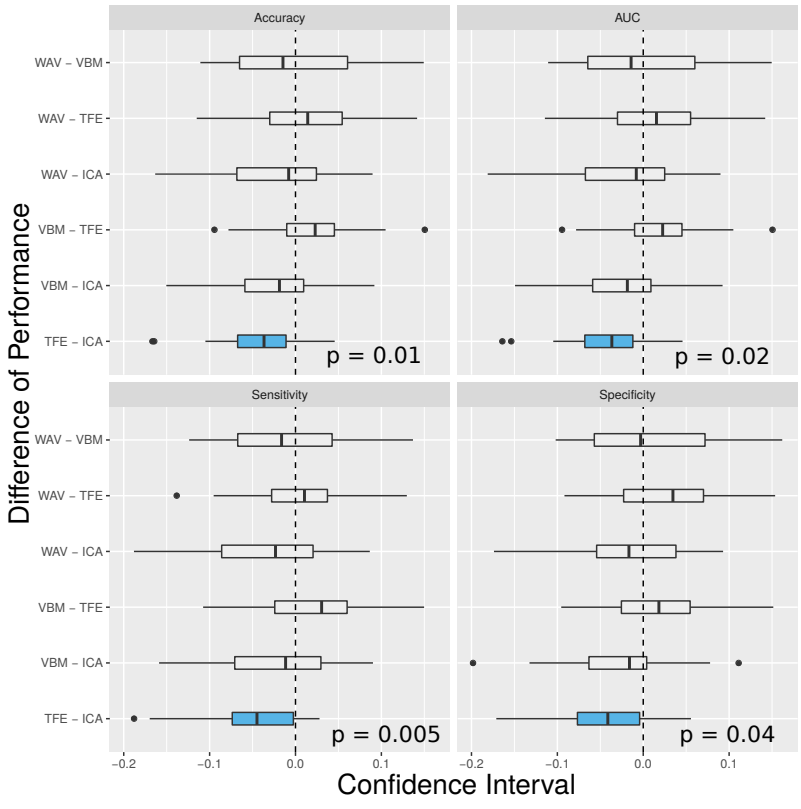

Figure 6.5 – SVM performance analysis for Open Access P300 Speller Database.

6.1.4 Comparison Between Classifiers

The best results obtained for the Open Acces P300 Speller database were:

1. LDA: using ICA, mean accuracy of 84.0% and standard deviation of 4.2%;
2. LOG: using ICA, mean accuracy of 83.8% and standard deviation of 3.8%;
3. SVM: using ICA, mean accuracy of 83.2% and standard deviation of 4.1%;

Table 6.4 summarizes the classification results using ICA with each of the classifiers. These results are also shown in the form of boxplots in Figure 6.6. Using the Friedman test to compare the results, no significant difference was found, meaning that the combinations of feature extraction technique and classifiers are statistically comparable.

Table 6.4 – Summary of classifier results for Open Access P300 Speller Database using ICA

Technique		**Acc. (%)**	**AUC (%)**	**Sens. (%)**	**Spec. (%)**
LDA	Median	83.4	83.4	82.8	84.6
	IQR	8.3	8.3	8.3	8.3
LOG	Median	**83.7**	**83.7**	**83.5**	**84.9**
	IQR	**5.8**	**5.8**	**7.3**	**4.4**
SVM	Median	82.4	82.4	82.2	83.0
	IQR	7.2	7.2	6.0	7.9

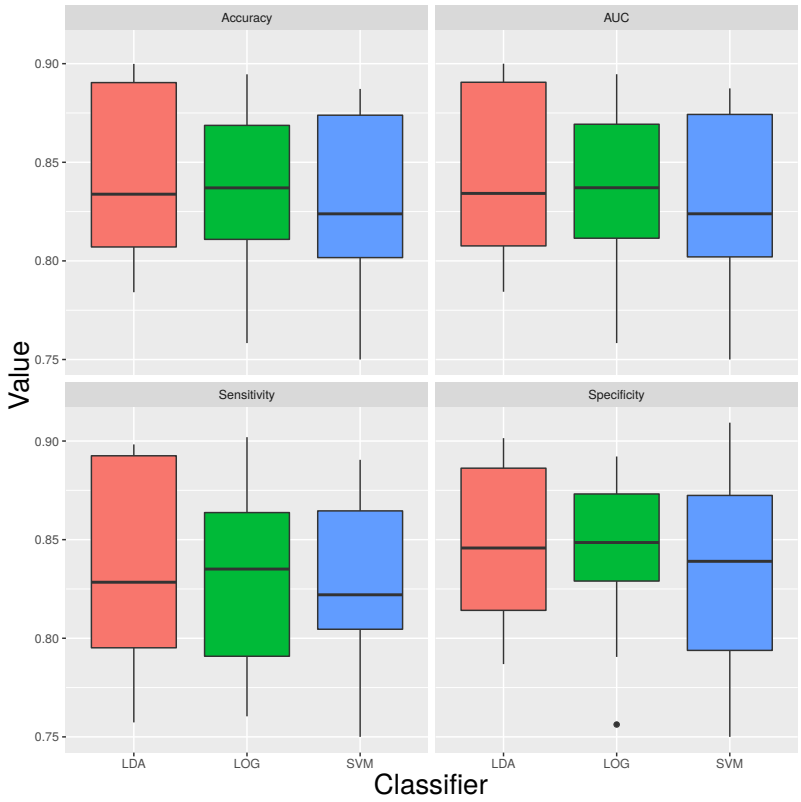

Figure 6.6 – Comparison of classifiers for Open Access P300 Speller Database.

6.2 Guger Database

This section describes the results obtained when the methods were applied on the Guger Database.

6.2.1 LDA Results

Table 6.5 summarizes the classification results obtained for each feature generation technique, using a LDA classifier. The best results were achieved using VBM, with a median accuracy of 78.4% and IQR of 7.5%. All of these results can be better visualized in the boxplots of Figure 6.7.

Friedman test indicated statistical differences with p-values of 0.001, 0.002, 0.005 and 0.003 for Acc, AUC, Sens and Spec respectively. The post-hoc analysis is illustrated in Figure 6.8 and indicated statistical difference between VBM and WAV.

Table 6.5 – Summary of LDA results for Guger Database

Technique		**Acc. (%)**	**AUC (%)**	**Sens. (%)**	**Spec. (%)**
ICA	Median	69.4	69.6	68.7	69.3
	IQR	4.8	4.8	5.1	4.3
TFE	Median	72.4	72.5	72.5	71.5
	IQR	10.4	10.6	11.2	9.6
VBM	Median	**78.4**	**78.4**	**77.0**	**79.0**
	IQR	**7.5**	**7.6**	**6.9**	**9.1**
WAV	Median	61.8	61.9	63.2	60.9
	IQR	6.6	6.7	5.8	6.3

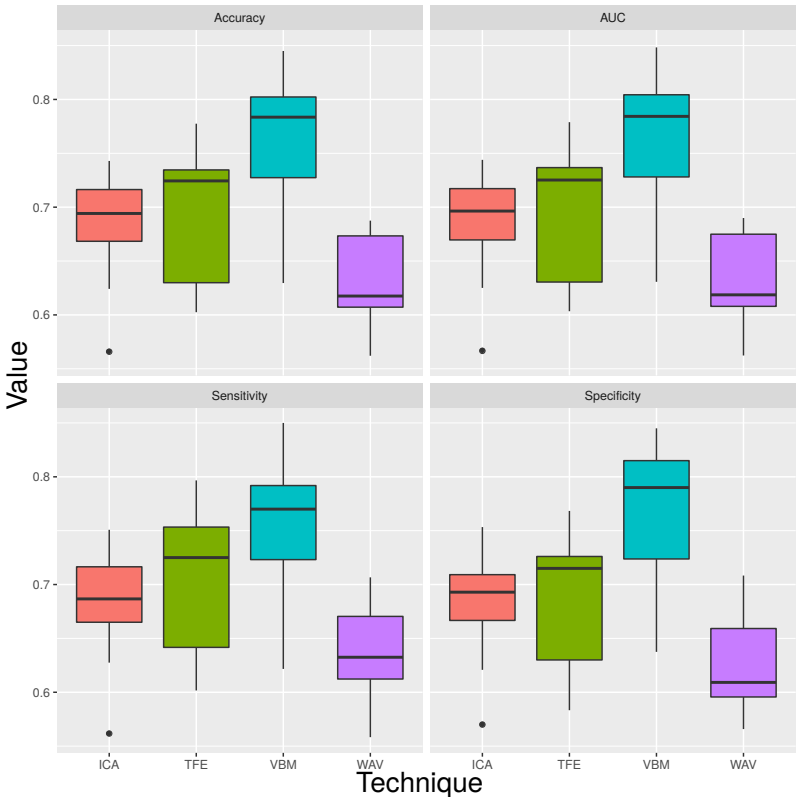

Figure 6.7 – LDA results for Guger Database.

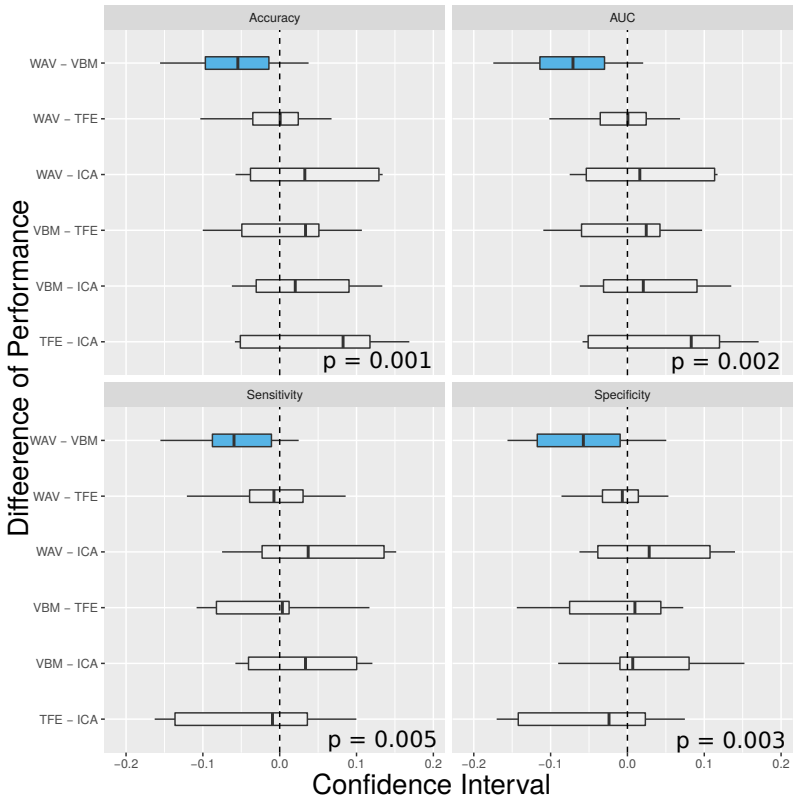

Figure 6.8 – LDA performance analysis for Guger Database.

6.2.2 LOG Results

Table 6.6 summarizes the classification results obtained using a LOG classifier. The best results were achieved using VBM, with a median accuracy of 77.0% and IQR of 7.7%. Figure 6.9 shows boxplots that summarize the metrics for each technique and all subjects.

When applying the Friedman test, statistical differences were found for Acc and AUC, with p-values of 0.02 for both metrics. The post-hoc analysis (Figure 6.10) showed statistical difference between VBM and WAV.

Table 6.6 – Summary of LOG results for Guger Database

Technique		**Acc. (%)**	**AUC (%)**	**Sens. (%)**	**Spec. (%)**
ICA	Median	74.2	73.0	73.3	74.2
	IQR	6.6	9.6	7.3	7.9
TFE	Median	72.9	72.4	75.8	68.8
	IQR	9.5	7.4	11.7	8.9
VBM	Median	**77.0**	**77.2**	**79.2**	**80.0**
	IQR	**7.7**	**4.4**	**11.7**	**6.0**
WAV	Median	72.3	74.3	72.0	73.3
	IQR	4.4	6.6	6.3	6.9

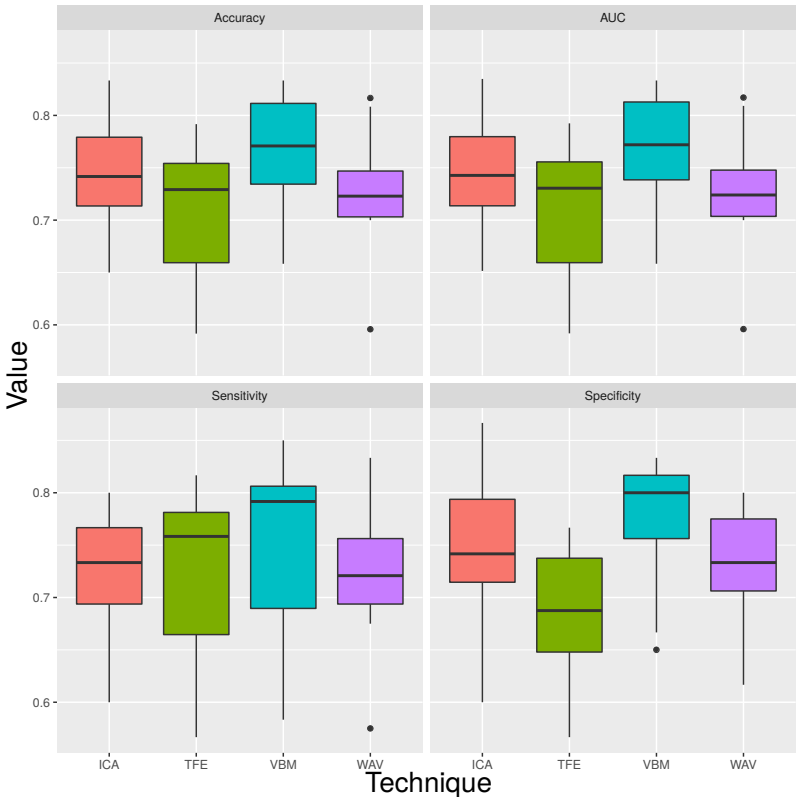

Figure 6.9 – LOG results for Guger Database.

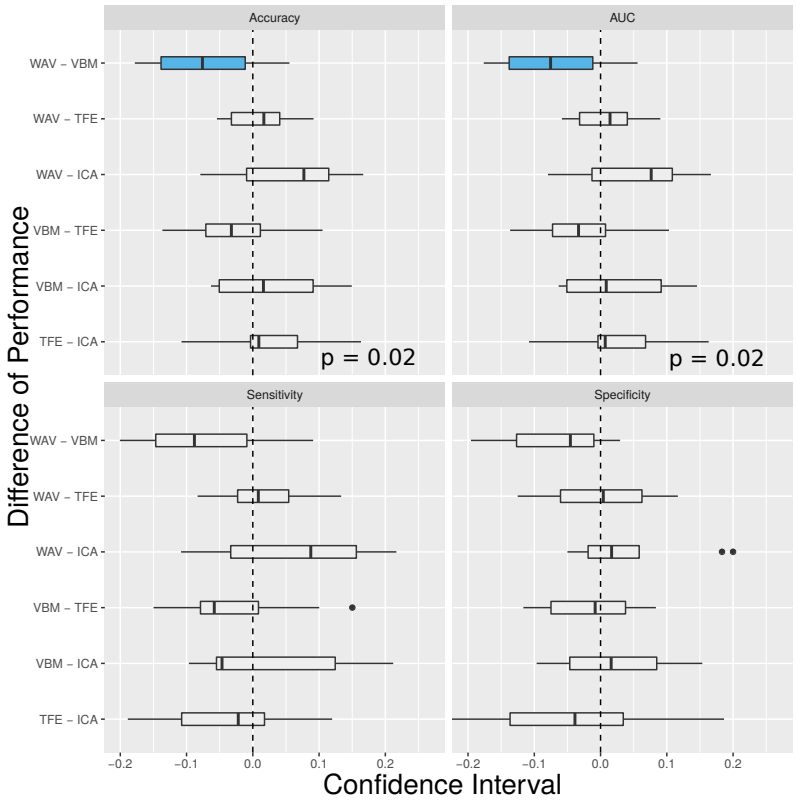

Figure 6.10 – LOG performance analysis for Guger Database.

6.2.3 SVM Results

Table 6.7 summarizes the classification results obtained using a SVM classifier. The best results were achieved using VBM, with a median accuracy of 77.7% and IQR of 7.0%. Figure 6.11 shows boxplots that summarize the metrics for each technique, considering all subjects.

The Friedman test revealed statistical differences between techniques for all metrics, with p-values of 0.02, 0.01, 0.03 and 0.04 for Acc AUC, Sens and Spec, respectively. The post-hoc analysis (Figure 6.12) identified statistical difference between VBM and WAV.

Table 6.7 – Summary of SVM results for Guger Database

Technique		**Acc. (%)**	**AUC (%)**	**Sens. (%)**	**Spec. (%)**
ICA	Median	76.3	76.2	75.0	77.5
	IQR	9.8	9.3	14.6	3.9
TFE	Median	72.3	72.3	68.3	71.7
	IQR	14.3	14.9	12.0	8.8
VBM	Median	**77.7**	**77.7**	**75.0**	**75.0**
	IQR	**7.0**	**7.0**	**12.1**	**5.0**
WAV	Median	66.9	67.3	65.8	70.4
	IQR	4.1	4.0	13.8	3.5

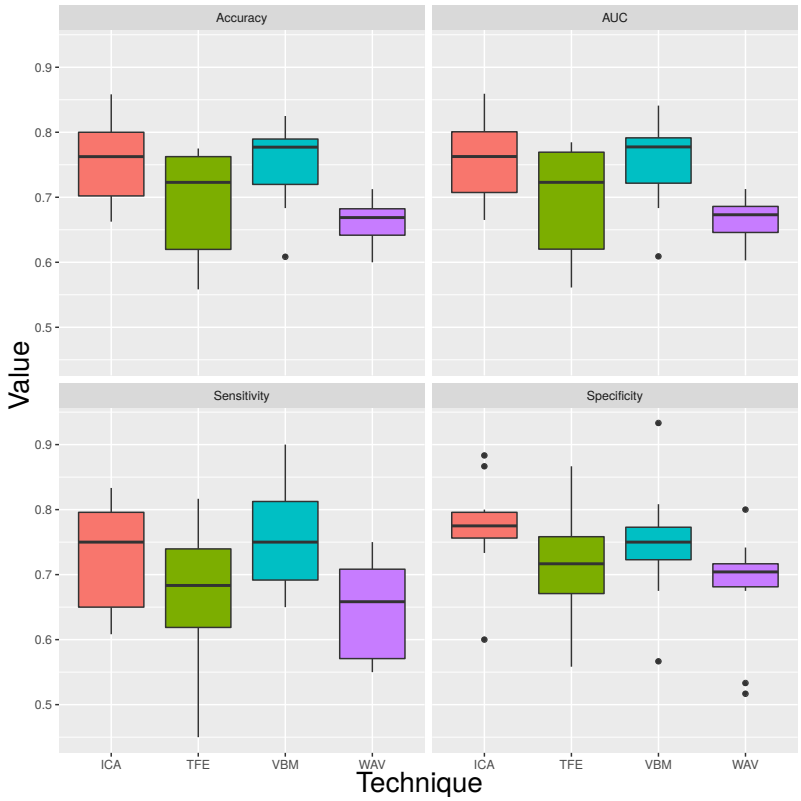

Figure 6.11 – SVM results for guger Database.

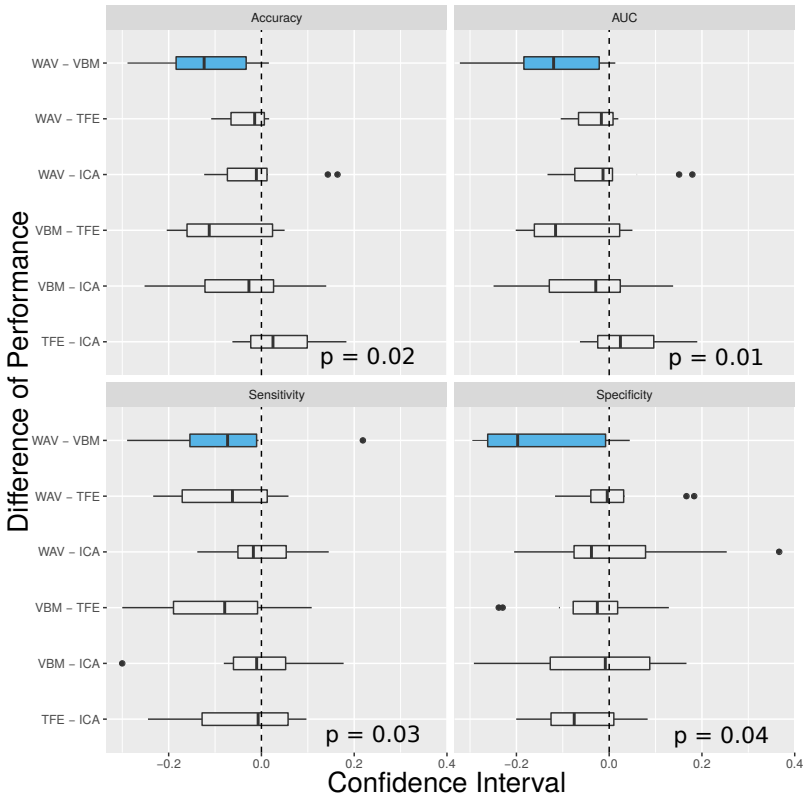

Figure 6.12 – SVM performance analysis for Guger Database.

6.2.4 Comparison Between Classifiers

The best results obtained for the Guger database were:

1. LDA: using VBM, mean accuracy of 75.6% and standard deviation of 7.0%;
2. LOG: using VBM, mean accuracy of 76.3% and standard deviation of 5.8%;
3. SVM: using VBM, mean accuracy of 75.3% and standard deviation of 6.6%;

Table 6.8 summarizes the classification results using VBM with each of the classifiers. These results are also shown in the form of boxplots in Figure 6.13. Using the Friedman test to compare the results, no significant difference was found, meaning that the combinations of feature extraction technique and classifiers are not statistically different.

Table 6.8 – Summary of classifier results for Guger database using VBM

Technique		**Acc. (%)**	**AUC (%)**	**Sens. (%)**	**Spec. (%)**
LDA	Median	**78.4**	**78.4**	**77.0**	**79.0**
	IQR	**7.5**	**7.6**	**6.9**	**9.1**
LOG	Median	77.0	77.2	77.2	70.0
	IQR	7.7	4.4	11.7	6.0
VBM	Median	77.7	77.7	75.0	75.0
	IQR	7.0	7.0	12.1	5.0

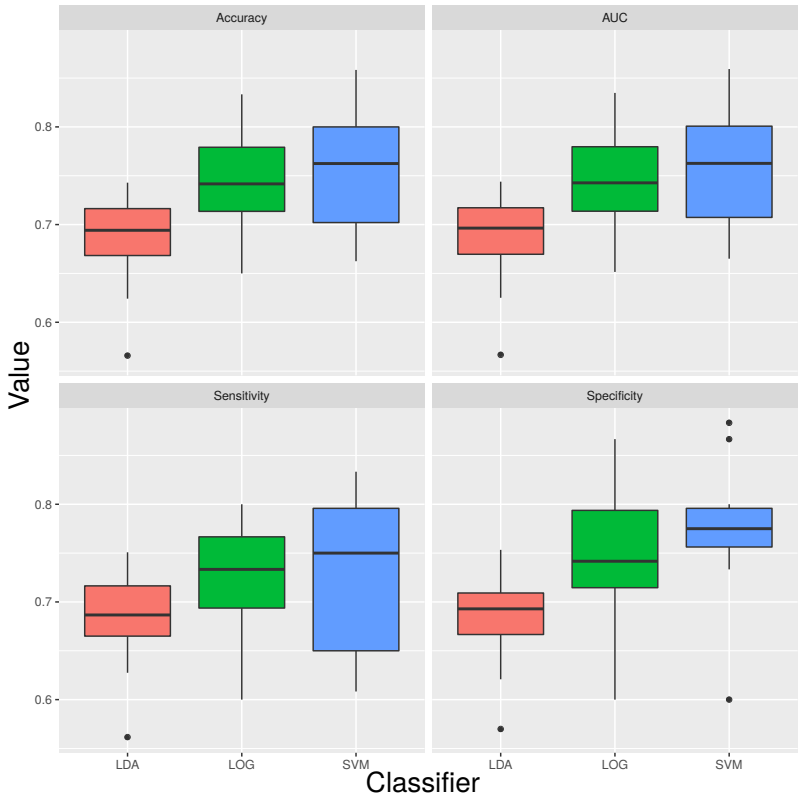

Figure 6.13 – Comparison of classifiers for Guger Database.

6.3 ALS Database

This section describes the results obtained when the methods were applied on the ALS Database.

6.3.1 LDA Results

Table 6.9 summarizes the classification results obtained for each feature generation technique, using a LDA classifier. The best results were achieved using VBM, with a median accuracy of 71.2% and IQR of 0.8%. Figure 6.14 shows boxplots that summarize the metrics for each of the techniques considering all subjects.

When the Friedman test was applied, statistical difference were found with p-values of 0.01, 0.01, 0.03 and 0.001 for Acc, AUC, Sens e Spec, respectively. The post-hoc analysis is illustrated in Figure 6.15 and indicates statistical difference between VBM and WAV and between VBM and TFE.

Table 6.9 – Summary of LDA results for ALS Database

Technique		**Acc. (%)**	**AUC (%)**	**Sens. (%)**	**Spec. (%)**
ICA	Median	70.6	70.6	70.2	70.8
	IQR	0.7	0.6	1.3	0.4
TFE	Median	65.7	65.8	67.0	64.8
	IQR	1.9	1.8	1.3	2.3
VBM	Median	**71.2**	**71.2**	**71.8**	**70.6**
	IQR	**0.8**	**0.9**	**1.3**	**0.7**
WAV	Median	62.7	62.7	62.2	62.7
	IQR	1.6	1.4	1.4	2.2

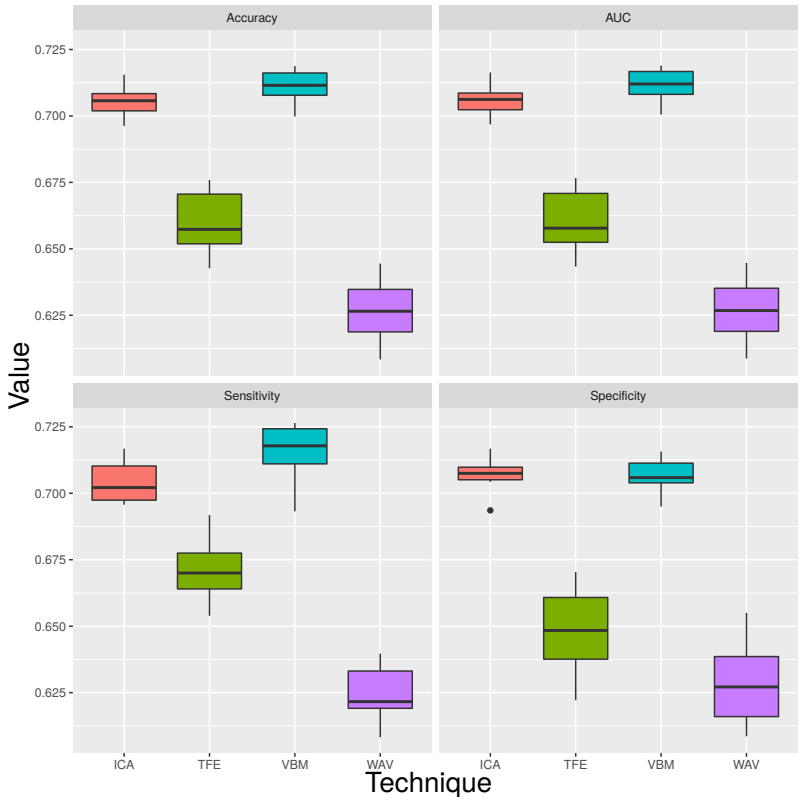

Figure 6.14 – LDA results for ALS Database.

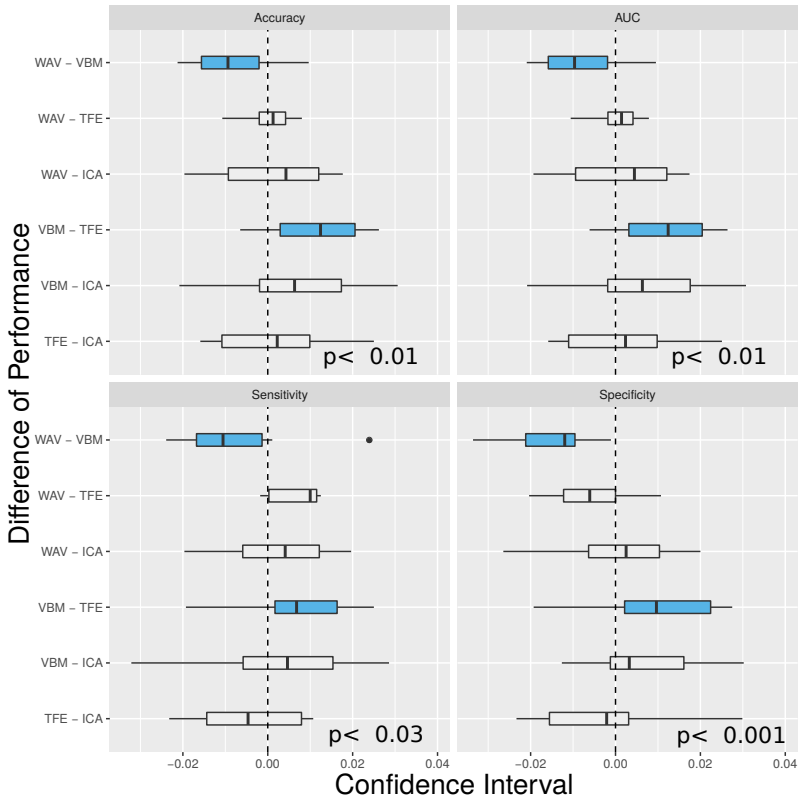

Figure 6.15 – LDA performance analysis for ALS Database.

6.3.2 LOG Results

Table 6.10 summarizes the classification results obtained using a LOG classifier. The best results were achieved using VBM, with a median accuracy of 70.0% and IQR of 3.1%. Figure 6.16 shows boxplots that summarize the metrics for each technique and all subjects.

Statistical differences were found with p-values of 0.03, 0.01, 0.01 and 0.01, respectively, for Acc, AUC, Sens and Spec. The post-hoc analysis (Figure 6.17) showed significant difference between VBM and TFE.

Table 6.10 – Summary of LOG results for ALS Database

Technique		**Acc. (%)**	**AUC (%)**	**Sens. (%)**	**Spec. (%)**
ICA	Median	69.8	69.8	70.4	70.4
	IQR	3.9	3.9	3.8	3.2
TFE	Median	67.3	67.4	69.6	64.1
	IQR	1.2	1.3	4.0	3.4
VBM	Median	**70.0**	**70.0**	**72.0**	**69.3**
	IQR	**3.1**	**3.2**	**4.3**	**3.4**
WAV	Median	69.1	69.2	69.8	67.7
	IQR	1.8	1.7	3.2	3.3

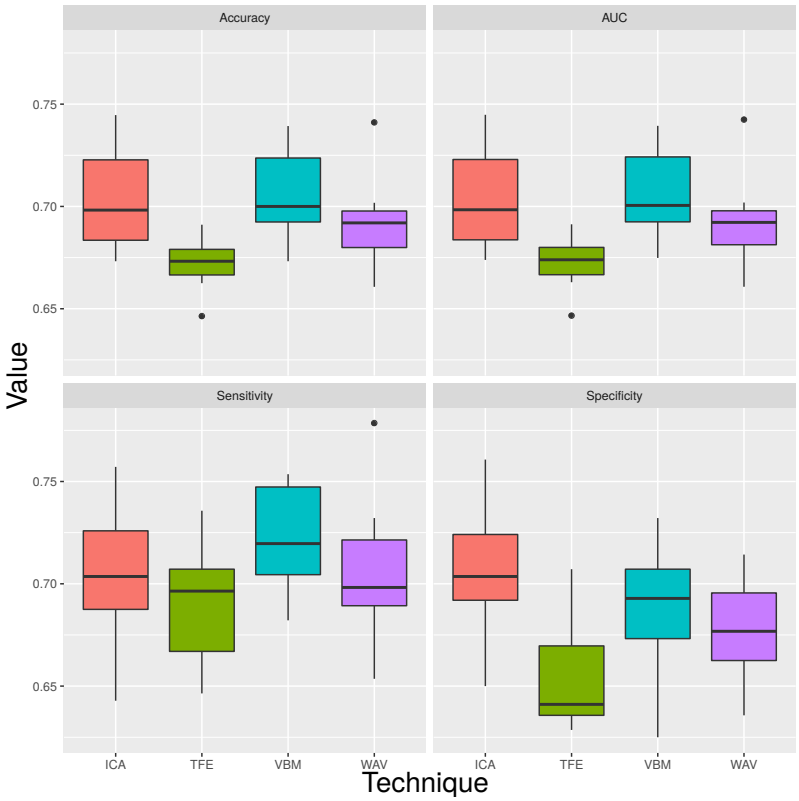

Figure 6.16 – LOG results for ALS Database.

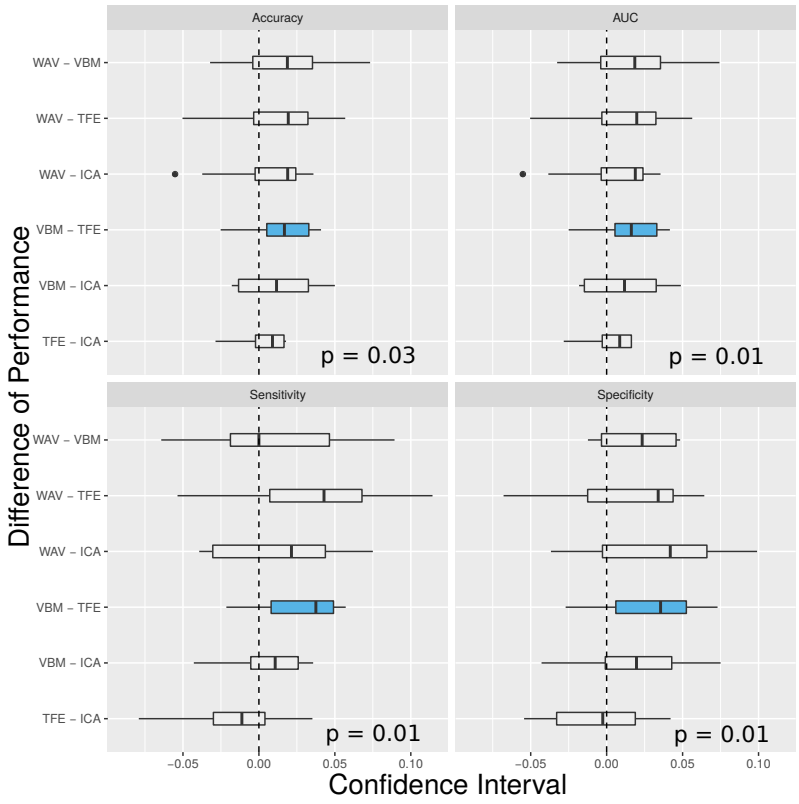

Figure 6.17 – LOG performance analysis for ALS Database.

6.3.3 SVM Results

Table 6.11 summarizes the classification results obtained using a SVM classifier. The best results were achieved using VBM, with a median accuracy of 72.0% and IQR of 1.7%. Figure 6.18 shows boxplots that summarize the metrics for each technique considering all subjects.

The Friedamn test indicated statistical differences with p-values of 0.001, 0.001, 0.03 and 0.009 for Acc, AUC, Sens and Spec, respectively. The post-hoc analysis (Figure 6.19) showed significant differences between VBM and WAV, ICA and WAV, VBM and TFE and ICA and TFE.

Table 6.11 – Summary of SVM results for ALS Database

Technique		**Acc. (%)**	**AUC (%)**	**Sens. (%)**	**Spec. (%)**
ICA	Median	70.6	70.7	71.1	71.3
	IQR	2.7	2.7	3.7	3.0
TFE	Median	67.1	67.2	67.1	65.7
	IQR	1.2	1.2	5.3	2.9
VBM	Median	**72.0**	**71.0**	**72.0**	**70.9**
	IQR	**1.7**	**1.7**	**3.2**	**1.8**
WAV	Median	66.3	66.3	65.7	67.7
	IQR	1.2	1.7	2.7	4.2

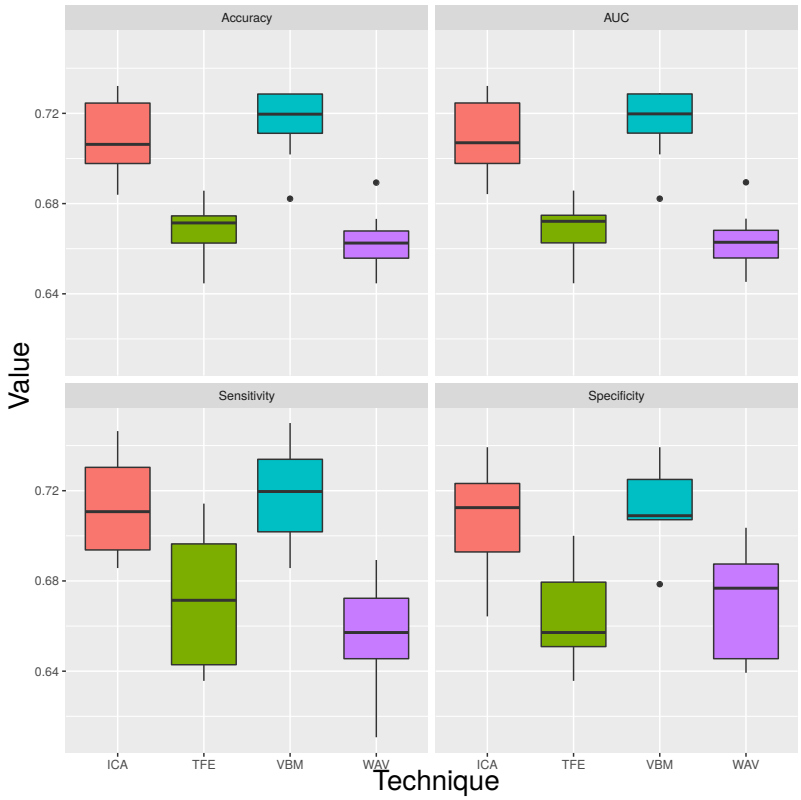

Figure 6.18 – SVM results for ALS Database.

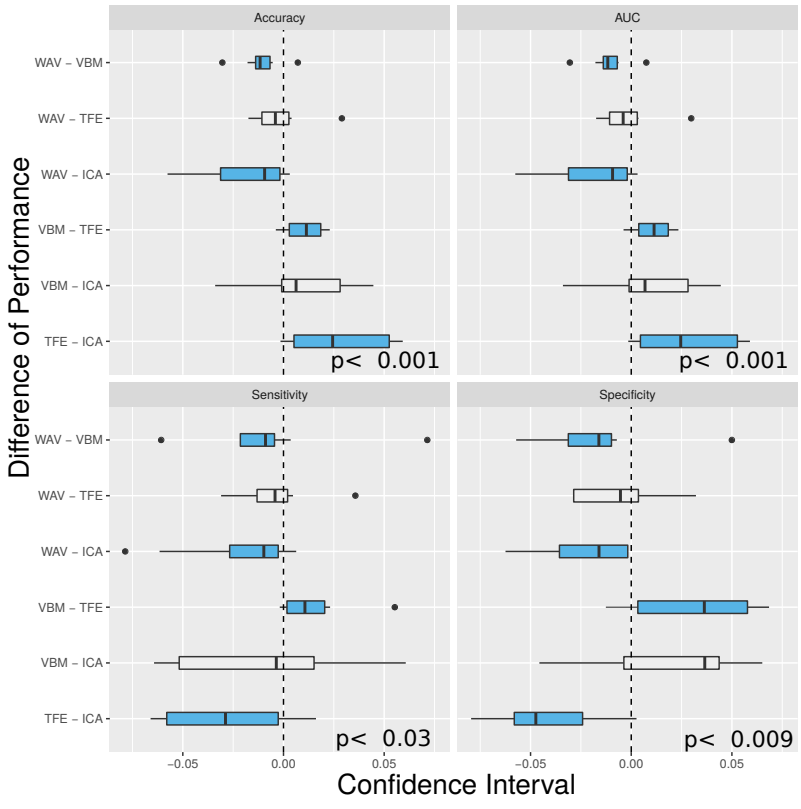

Figure 6.19 – SVM performance analysis for ALS Database.

6.3.4 Comparison Between Classifiers

The best results obtained for the ALS database were:

1. LDA: using VBM, mean accuracy of 71.1% and standard deviation of 0.7%;
2. LOG: using VBM, mean accuracy of 70.6% and standard deviation of 2.2%;
3. SVM: using VBM, mean accuracy of 71.5% and standard deviation of 1.6%;

Table 6.12 summarizes the classification results using VBM with each of the classifiers. These results are also shown in the form of boxplots inf Figure 6.20. Using the Friedman test to compare the results, no significant difference was found, meaning that the combinations of feature extraction technique and classifiers are statistically comparable.

Table 6.12 – Summary of classifier results for ALS database using VBM

Technique		**Acc. (%)**	**AUC (%)**	**Sens. (%)**	**Spec. (%)**
LDA	Median	71.2	71.2	71.8	70.6
	IQR	0.8	0.9	1.3	0.7
LOG	Median	70.0	70.0	72.0	69.3
	IQR	3.1	3.2	4.3	3.4
SVM	Median	**72.0**	**71.0**	**72.0**	**70.9**
	IQR	**1.7**	**1.7**	**3.2**	**1.8**

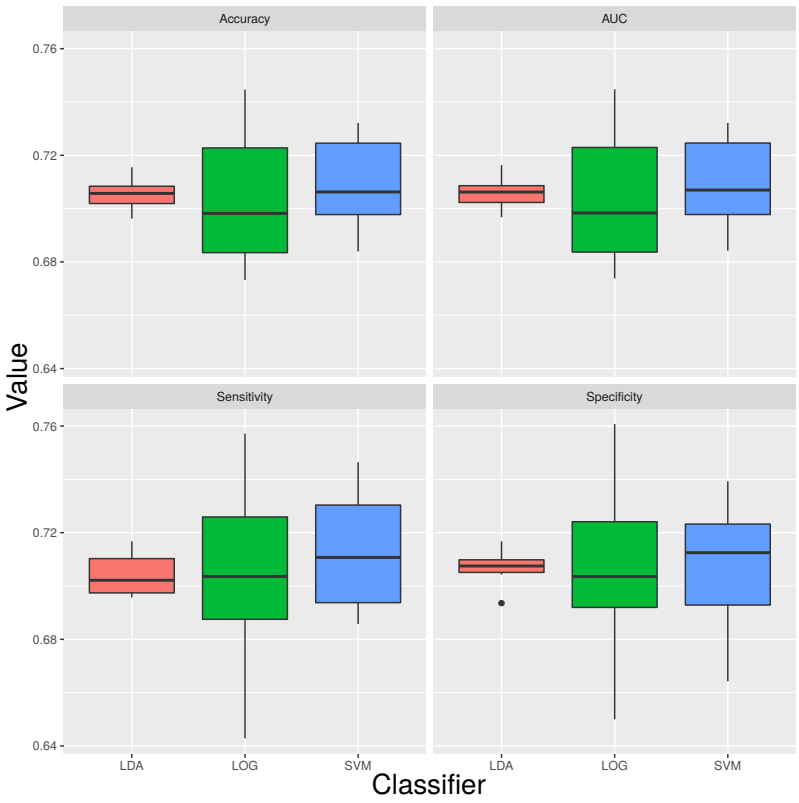

Figure 6.20 – Comparison of classifiers for ALS database.

7 Discussion

In this chapter, the results obtained in this dissertation are discussed. A general discussion of the meaning of the results is given, followed by comparisons with recent literature results.

7.1 General Discussion

As cited by Cecotti e Ries (2017), single-trial P300 detection is not a trivial task to execute. Efficient single-trial detection methods require many processing steps, including artifact removal, spatio-temporal filtering and classification.

Several obstacles arise when trying to perform single-trial P300 detection. Users can be distracted from the given BCI-task, becoming tired or simply losing interest, resulting in misclassification problems (JANSEN *et al.*, 2004).

Considered together, these factors impose several difficulties to perform single-trial detection with elevated accuracy rates, possibly precluding methods of consistently achieving above 80%, as stated by Magee e Givigi (2015b). Moreover, efficient methods should consist of simple and robust algorithms, requiring functions with as few parameters as possible, to facilitate adjustment for a vast number of users (CECOTTI; RIES, 2017).

The methods proposed in this work extracted different features from raw EEG data using a variety of metrics which involves time, frequency, time-frequency and statistical parameters, therefore enhancing the separation between *target* and *non-target* signals.

The parameters extracted by the signal processing techniques, used to fed simple, yet efficient classifiers such as linear discriminant analysis and logistic models, achieved consistent accuracies in the range of 75% to 85%, which are very good percentages for nowadays real life applications (W; DONCHIN, 2006).

Furthermore, the methods proposed are simple enough to be applied with no special requirements of computational power and/or inter-individual adjustment.

While single-trial detection was successfully achieved, it is important to notice that they can also be employed in double-trial and variable-trial (where the number of epochs can be adequate dynamically).

7.2 Comparison Between Techniques

The objective of this dissertation was to investigate what are the best combination of feature extraction technique and classifier to perform single-trial P300 detection. Two techniques were noteworthy: independent component analysis and variance-based metrics.

While ICA achieved the highest overall results for the Open Access Database, VBM presented the best results considering all the databases, which indicates a higher level of robustness. Regarding the classifiers, no statistical differences were found between linear discriminant analysis, logistic models and support vector machines.

Therefore, the choice of a simpler model like LDA or LOG is indicated. Besides having fewer parameters and being relatively easy to implement, the training of these methods is simple, requiring less time for an invidual to begin using the BCI.

Finally, it is important to notice that VBM performed better in the ALS database, which may be due to the fact that VBM is less affected by changes in the P300 waveform, as it relies on the statistical distribution of the ERP. This robustness advocates in favor of its use in real life applications.

7.3 Comparison With Literature Results

A comparison between the results achieved in this dissertation and recent literature works focused on single-trial P300 is shown in Table 7.1, considering the best combination of feature extraction technique and classifier obtained for each database. One can notice that the results obtained for the three databases are comparable with the recent results reported in the literature.

For the Open Access Database (which contains signals recorded from 24 healthy subjects), the result is close to the one achieved by Li *et al.* (2012) (with 5 healthy subjects), despite being evaluated here with a far greater number of subjects. Apart from Li *et al.* (2012), it is better than any other work reported in Table 7.1.

Regarding the Guger database, the results are better than the majority of the other papers (except than the same work of Li *et al.* (2012)), also indicating the strength of the proposed methods.

Even the performance for the ALS database, for which we obtained worse results than for healthy subjects (SILVONI *et al.*, 2009), it was comparable to the results reported from works with healthy people (Table 7.1).

Table 7.1 – Comparison of dissertation and literature results for single-trial P300 detection

Paper	Subjects	Accuracy (%)	Methods
This dissertation, Open Access Database	**24**	**84.0**	**EEG Time Samples; ICA; SVM**
This dissertation, Guger Database	**10**	**76.3**	**Variance-based metrics; LOG**
This dissertation, ALS Database	**8**	**71.5**	**Variance-based metrics; SVM**
Lenhardt, Kaper e Ritter (2008)	12	65.5	EEG Time Samples; PCA; LDA
Finke, Lenhardt e Ritter (2009)	11	65.0	EEG Time Samples; PCA; FLDA
Li *et al.* (2009)	1	76.7	EEG Time Samples; ICA
Li *et al.* (2012)	5	84.8	D metrics; Threshold Detection
Haghighatpanah *et al.* (2013)	2	65.0	Discrete Wavelets; ICA; LDA
Morales *et al.* (2014)	10	61.2	Features extracted from P300 peak; SOM Neural Network
Vareka e Mautner (2015)	5	72.8	Windowed Means; LDA
Magee e Givigi (2015b)	3	76.4	EEG Time Samples; Genetic Algorithm; Neural Network
Wu *et al.* (2016)	2	70.0	EEG Time Samples; Least-Angle Regression; Sparse LDA

It is important to notice that the methods proposed in this dissertation were validated across different databases and, moreover, with a number of subjects that is far greater than the results presented in the literature.

This indicates that, besides the fact that the methods achieved very good results, they are also very robust to the highly variable P300 waveform. In comparison with works that used a similar number of subjects (LENHARDT; KAPER; RITTER, 2008; FINKE; LENHARDT; RITTER, 2009; MORALES *et al.*, 2014), the methods proposed in this dissertation present better results.

8 Conclusion

In this chapter, the concluding remarks drawn from the dissertation are presented, as well as suggestios for future work.

The purpose of this dissertation was to investigate different feature extraction techniques and classifiers, with the final objective to perform single-trial P300 detection.

Four feature extraction techniques – Independent Component Analysis, Time and Frequency Extracted Parameters, Variance-based Metrics and Wavelet Coefficients – as well as three different classifiers – Linear Discriminant Analysis, Logistic Models and Support Vector Machines – were used to categorize data into two classes, P300 signals and single EEG epochs.

Three databases were employed to test the investigated methods, two consisting of healthy subjects and one consisting of subjects that suffer from ALS. All combinations of investigated techniques were able to correctly detect single trial P300.

No significant difference was found between the classifiers, indicating the use of more simple classifiers, such as LDA and LOG, could be suitable.

Regarding feature extraction techniques, ICA and VBM achieved the best results, considering all databases, reaching mean single-trial detection accuracies up to 84% and 80%, respectively.

While ICA achieved higher accuracies, VBM appears to be more robust regarding waveform variation and performed better in ALS patients.

Moreover, VBM is a simple and elegant technique that requires little processing (computational) power to calculate features, what is very important to real-time BCI, since, in these applications, one wishes to minimize the time required to train the BCI.

As future works, we suggest:

- To investigate the use of double-trial and variable-trial detection, employing thresholds of detection probability for accuracy enhancing;
- To combine the here study classification methods in order to improve detection rates, once each feature extraction technique and classifier could have a strength regarding the focused parameters (time, frequency or statistical structure);

- Apply the methods developed in this dissertation in real-time applications.

Bibliography

ALHADDAD, M. J. Common Average Reference (CAR) Improves P300 Speller. *International Journal of Engineering and Technology*, v. 2, n. 3, p. 451–465, 2012. Disponível em: <http://iet-journals.org/archive/2012/march_vol_2_no_3/381359132985477.pdf>. Cited on page 26.

ALHADDAD, M. J.; KAMEL, M.; MALIBARY, H.; THABIT, K.; DAHLWI, F.; HADI, A. P300 speller efficiency with common average reference. In: *Proceedings of the Third international conference on Autonomous and Intelligent Systems*. [s.n.], 2012. p. 234–241. Disponível em: <http://link.springer.com/chapter/10.1007/978-3-642-31368-4_28>. Cited on page 26.

ALLISON, B. Z.; PINEDA, J. A. ERPs evoked by different matrix sizes: implications for a brain-computer interface (BCI) system. *IEEE Transactions on Neural Systems and Rehabilitation Engineering*, v. 11, n. 2, p. 110–113, 2003. Disponível em: <http://dx.doi.org/10.1109/tnsre.2003.814448>. Cited on page 1.

ALOISE, F.; SCHETTINI, F.; ARICÒ, P.; SALINARI, S.; GUGER, C.; RINSMA, J.; AIELLO, M.; MATTIA, D.; CINCOTTI, F. Asynchronous p300-based brain-computer interface to control a virtual environment: initial tests on end users. *Clinical EEG and Neuroscience*, v. 42, n. 4, p. 219–224, 2011. Disponível em: <http://eeg.sagepub.com/content/42/4/219.short>. Cited 2 times on pages 20 and 21.

BASHASHATI, A.; FATOURECHI, M.; WARD, R. K.; BIRCH, G. E. A survey of signal processing algorithms in brain-computer interfaces based on electrical brain signals. *Journal of Neural Engineering*, v. 4, n. 2, p. R32, 2007. Disponível em: <http://stacks.iop.org/1741-2552/4/i=2/a=R03>. Cited 2 times on pages 1 and 19.

BAYLISS, J. D. Use of the evoked potential p3 component for control in a virtual apartment. *Neural Systems and Rehabilitation Engineering, IEEE Transactions on*, v. 11, n. 2, p. 113–116, 2003. Disponível em: <http://dx.doi.org/10.1109/TNSRE.2003.814438>. Cited 2 times on pages 20 and 21.

BAYLISS, J. D.; BALLARD, D. H. Single trial p300 recognition in a virtual environment. In: *University of Rochester*. [s.n.], 1999. p. 22–25. Disponível em: <http://vrlab.cps.utexas.edu/papers/scb99.pdf>. Cited 2 times on pages 20 and 21.

BLACKWOOD, W. J. M. D. H. Cognitive brain potentials and their application. *The British Journal of Psychiatry*, v. 157, n. 1, p. 96 – 101, 1990. Disponível em: <http://www.ncbi.nlm.nih.gov/pubmed/2291824>. Cited on page 9.

BOSER, B. E.; GUYON, I. M.; VAPNIK, V. N. A training algorithm for optimal margin classifiers. In: *Proceedings of the Fifth Annual Workshop on Computational Learning Theory*. ACM, 1992. p. 144–152. Disponível em: <http://doi.acm.org/10.1145/130385.130401>. Cited on page 40.

BOSTANOV, V.; KOTCHOUBEY, B. The t-cwt: a new erp detection and quantification method based on the continuous wavelet transform and student's

t-statistics. *Clinical Neurophysiology*, v. 117, n. 12, p. 2627–2644, 2006. Disponível em: <http://dx.doi.org/10.1016/j.clinph.2006.08.012>. Cited on page 9.

BOUGRAIN C. SAAVEDRA, R. R. L. Finally, what is the best filter for p300 detection? In: *Proceedings of the TOBI Workshop III - Tools for Brain-Computer Interaction*. [s.n.], 2012. Disponível em: <http://hal.archives-ouvertes.fr/docs/00/75/66/69/PDF/Bougrain-TobiWorkshop12Final.pdf>. Cited on page 25.

BROUWER, A.-M.; ERP, J. B. F. van. An auditory oddball (P300) spelling system for brain-computer interfaces. *Frontiers in Neuroscience*, v. 4, 2010. Disponível em: <http://www.ncbi.nlm.nih.gov/pmc/articles/PMC2871714/>. Cited on page 19.

BURGES, C. J. A tutorial on support vector machines for pattern recognition. *Data Mining and Knowledge Discovery*, v. 2, p. 121–167, 1998. Disponível em: <http://dl.acm.org/citation.cfm?id=593463>. Cited 2 times on pages 40 and 42.

CECOTTI, H. Toward shift invariant detection of event-related potentials in non-invasive brain-computer interface. *Pattern Recognition Letters*, v. 66, p. 127–134, 2015. Disponível em: <http://dx.doi.org/10.1016/j.patrec.2015.01.015>. Cited on page 9.

CECOTTI, H.; RIES, A. J. Best practice for single-trial detection of event-related potentials: Application to brain-computer interfaces. *International Journal of Psychophysiology*, v. 111, p. 156–169, 2017. Disponível em: <http://dx.doi.org/10.1016/j.ijpsycho.2016.07.500>. Cited on page 75.

CEDARBAUM, J. M.; STAMBLER, N.; MALTA, E.; FULLER, C.; HILT, D.; THURMOND, B.; NAKANISHI, A.; GROUP, B. A. S.; GROUP, A. complete listing of the B. S. *et al.* The alsfrs-r: a revised als functional rating scale that incorporates assessments of respiratory function. *Journal of the neurological sciences*, v. 169, n. 1, p. 13–21, 1999. Disponível em: <http://dx.doi.org/10.1016/S0022-510X(99)00210-5>. Cited on page 45.

CHUI, C. K. *An introduction to wavelets*. [S.l.]: Academic press, 2014. v. 1. Cited on page 34.

COMERCHERO, M. D.; POLICH, J. P3a and p3b from typical auditory and visual stimuli. *Clinical Neurophysiology*, v. 110, p. 24–30, 1999. Disponível em: <http://www.ncbi.nlm.nih.gov/pubmed/10348317>. Cited on page 13.

COMON, P. Independent component analysis, a new concept? *Signal Processing*, v. 36, n. 3, p. 287–314, 1994. Disponível em: <http://dx.doi.org/10.1016/0165-1684(94)90029-9>. Cited 2 times on pages 26 and 27.

CORTES, C.; VAPNIK, V. Support-vector networks. *Machine Learning*, v. 20, n. 3, p. 273–297, 1995. Disponível em: <http://dx.doi.org/10.1023/A:1022627411411>. Cited 2 times on pages 40 and 41.

COVER, T. M.; THOMAS, J. A. *et al. Elements of information theory*. [S.l.]: Wiley, 1991. Cited on page 30.

DAUBECHIES, I. *et al. Ten lectures on wavelets*. [S.l.]: SIAM, 1992. v. 61. Cited on page 36.

DAVIES, P. L.; GAVIN, W. J. Validating the diagnosis of sensory processing disorders using eeg technology. *The American journal of occupational therapy*, v. 61, n. 2, p. 176, 2007. Disponível em: <http://search.proquest.com/openview/ecb5679ae26ea993e55967aa944aa1db>. Cited on page 9.

DELORME, A.; MAKEIG, S.; SEJNOWSKI, T. Automatic artifact rejection for eeg data using high-order statistics and independent component analysis. In: *Proc. of the 3rd International Workshop on ICA*. [S.l.: s.n.], 2001. v. 457, p. 462. Cited on page 25.

DEMŠAR, J. Statistical comparisons of classifiers over multiple data sets. *Journal of Machine learning research*, v. 7, n. Jan, p. 1–30, 2006. Disponível em: <http://citeseer.ist.psu.edu/viewdoc/summary?doi=10.1.1.141.31425>. Cited on page 51.

DIETRICH, A.; KANSO, R. A review of EEG, ERP, and neuroimaging studies of creativity and insight. *Psychology Bulletin*, v. 136, n. 5, p. 822–848, 2010. Disponível em: <http://www.ncbi.nlm.nih.gov/pubmed/20804237>. Cited 2 times on pages 1 and 5.

DUDA, R. O.; HART, P. E.; STORK, D. G. *Pattern classification*. [S.l.]: John Wiley & Sons, 2012. Cited on page 37.

ELSHOUT, J.; MOLINA, G. G. *Review of brain-computer interfaces based on the P300 evoked potential*. Philips Research Europe, 2009. Disponível em: <dspace.library.uu.nl/handle/1874/33417>. Cited on page 16.

FABIANI, M.; GRATTON, G.; KARIS, D.; DONCHIN, E. Definition, identification, and reliability of measurement of the p300 component of the event-related brain potential. *Advances in Psychophysiology*, v. 2, p. 1, 1987. Disponível em: <http://scholarcommons.usf.edu/psy_facpub/286/>. Cited on page 16.

FARWELL, L. A.; DONCHIN, E. Talking off the top of your head: Toward a mental prosthesis utilizing event-related brain potentials. *Electroencephalography and Clinical Neurophysiology*, v. 70, p. 510–523, 1988. Disponível em: <http://www.ncbi.nlm.nih.gov/pubmed/2461285>. Cited 4 times on pages 13, 14, 19, and 25.

FINKE, A.; LENHARDT, A.; RITTER, H. The mindgame: a p300-based brain–computer interface game. *Neural Networks*, v. 22, n. 9, p. 1329–1333, 2009. Disponível em: <http://www.sciencedirect.com/science/article/pii/S0893608009001579>. Cited 3 times on pages 21, 22, and 77.

FURDEA, A.; HALDER, S.; KRUSIENSKI, D. J.; BROSS, D.; NIJBOER, F.; BIRBAUMER, N.; KüBLER, A. An auditory oddball (P300) spelling system for brain-computer interfaces. *Psychophysiology*, v. 46, n. 3, p. 617–625, 2009. Disponível em: <http://www.ncbi.nlm.nih.gov/pubmed/19170946>. Cited on page 19.

GUGER, C.; DABAN, S.; SELLERS, E.; HOLZNER, C.; KRAUSZ, G.; CARABALONA, R.; GRAMATICA, F.; EDLINGER, G. How many people are able to control a p300-based brain–computer interface (bci)? *Neuroscience letters*, v. 462, n. 1, p. 94–98, 2009. Disponível em: <http://www.sciencedirect.com/science/article/pii/S0304394009008192>. Cited 2 times on pages 20 and 44.

GUGER, C.; EDLINGER, G.; HARKAM, W.; NIEDERMAYER, I.; PFURTSCHELLER, G. How many people are able to operate an EEG-based brain-computer interface (BCI)? *IEEE Transactions on Neural Systems and Rehabilitation Engineering*, v. 11, n. 2, p.

145–147, 2003. Disponível em: <dx.doi.org/10.1109/TNSRE.2003.814481>. Cited on page 20.

HAGHIGHATPANAH, N.; AMIRFATTAHI, R.; ABOOTALEBI, V.; NAZARI, B. A single channel-single trial p300 detection algorithm. In: *2013 21st Iranian Conference on Electrical Engineering (ICEE)*. [s.n.], 2013. p. 1–5. Disponível em: <http://dx.doi.org/10.1109/IranianCEE.2013.6599576>. Cited 3 times on pages 22, 23, and 77.

HERRMANN, C. S.; MUNK, M. H.; ENGEL, A. K. Cognitive functions of gamma-band activity: memory match and utilization. *Trends in cognitive sciences*, Elsevier, v. 8, n. 8, p. 347–355, 2004. Cited on page 7.

HUGGINS, J. E.; LEVINE, S. P.; BEMENT, S. L.; KUSHWAHA, R. K.; SCHUH, L. A.; PASSARO, E. A.; ROHDE, M. M.; ROSS, D. A.; ELISEVICH, K. V.; SMITH, B. J. Detection of event-related potentials for development of a direct brain interface. *Journal of Clinical Neurophysiology*, v. 16, n. 5, p. 448, 1999. Disponível em: <http://journals.lww.com/clinicalneurophys/toc/1999/09000>. Cited on page 9.

HUGHES, J. R. Gamma, fast, and ultrafast waves of the brain: Their relationships with epilepsy and behavior. *Epilepsy and Behavior*, v. 13, n. 1, p. 25 – 31, 2008. Disponível em: <http://dx.doi.org/10.1016/j.yebeh.2008.01.011>. Cited on page 6.

HWANG, H.-J.; KWON, K.; IM, C.-H. Neurofeedback-based motor imagery training for brain–computer interface (bci). *Journal of Neuroscience Methods*, Elsevier, v. 179, n. 1, p. 150–156, 2009. Disponível em: <http://dx.doi.org/10.1016/j.jneumeth.2009.01.015>. Cited on page 1.

HYVARINEN, A.; OJA, E. Independent component analysis: Algorithms and applications. *Neural Networks*, v. 13, n. 3, p. 411–430, 2000. Disponível em: <http://www.ncbi.nlm.nih.gov/pubmed/10946390>. Cited 5 times on pages 26, 27, 28, 29, and 31.

ITURRATE, I.; ANTELIS, J. M.; KUBLER, A.; MINGUEZ, J. A noninvasive brain-actuated wheelchair based on a p300 neurophysiological protocol and automated navigation. *IEEE Transactions on Robotics*, IEEE, v. 25, n. 3, p. 614–627, 2009. Cited on page 21.

JANSEN, B. H.; ALLAM, A.; KOTA, P.; LACHANCE, K.; OSHO, A.; SUNDARESAN, K. An exploratory study of factors affecting single trial p300 detection. *IEEE transactions on Biomedical Engineering*, v. 51, n. 6, p. 975–978, 2004. Disponível em: <https://doi.org/10.1109/TBME.2004.826684>. Cited on page 75.

JASPER, H. H. Report of the Committee on Methods of Clinical Examination in Electroencephalography. *Electroencephalography and Clinical Neurophysiology*, v. 10, n. 2, p. 370 – 375, 1958. Disponível em: <http://dx.doi.org/10.1016/0013-4694(58)90053-1>. Cited on page 7.

KAPER, M.; MEINICKE, P.; GROSSEKATHÖFER, U.; LINGNER, T.; RITTER, H. Bci competition 2003-data set iib: support vector machines for the p300 speller paradigm. *IEEE Transactions on Biomedical Engineering*, v. 51, n. 6, p. 1073–1076, 2004. Disponível em: <http://www.ncbi.nlm.nih.gov/pubmed/15188881>. Cited on page 42.

KLASS, D. W. The continuing challenge of artifacts in the eeg. *American Journal of EEG Technology*, v. 35, n. 1, p. 239 – 269, 1995. Disponível em: <http://www.msetinfo.org/pdf/The_Continuous_Challenge_of_Artifacts_in_the_EEG_1_.pdf>. Cited on page 8.

KÜBLER, A.; HALDER, S.; FURDEA, A.; HÖSLE, A. Brain painting-bci meets art. In: *Proceedings of the 4th International Brain-Computer Interface Workshop and Training Course*. [S.l.: s.n.], 2008. p. 361–366. Cited 2 times on pages 20 and 21.

LEDESMA-RAMIREZ, C.; BOJORGES-VALDEZ, E.; YÁÑEZ-SUAREZ, O.; SAAVEDRA, C.; BOUGRAIN, L.; GENTILETTI, G. G. *et al.* An open-access p300 speller database. In: *Fourth International Brain-Computer Interface Meeting*. [s.n.], 2010. Disponível em: <http://hal.inria.fr/inria-00549242/en>. Cited on page 43.

LEHMANN, E. L.; ROMANO, J. P. *Testing statistical hypotheses*. [S.l.]: Springer Science & Business Media, 2006. Cited 2 times on pages 50 and 51.

LENHARDT, A.; KAPER, M.; RITTER, H. J. An adaptive p300-based online brain–computer interface. *IEEE Transactions on Neural Systems and Rehabilitation Engineering*, v. 16, n. 2, p. 121–130, 2008. Disponível em: <http://dx.doi.org/10.1109/TNSRE.2007.912816>. Cited 2 times on pages 22 and 77.

LI, K. *Advanced Signal Processing Techniques for Single Trial Electroencephalography Signal Classification for Brain Computer Interface Applications*. Tese (Doutorado) — University of South Florida, 2010. Disponível em: <http://scholarcommons.usf.edu/etd/3484>. Cited 3 times on pages 27, 32, and 33.

LI, K.; SANKAR, R.; ARBEL, Y.; DONCHIN, E. Single trial independent component analysis for p300 bci system. In: *Engineering in Medicine and Biology Society, 2009. EMBC 2009. Annual International Conference of the IEEE*. [s.n.], 2009. p. 4035–4038. Disponível em: <http://dx.doi.org/10.1109/IEMBS.2009.5333745>. Cited 2 times on pages 22 and 77.

LI, K.; SANKAR, R.; CAO, K.; ARBEL, Y.; DONCHIN, E. A new single trial p300 classification method. *International Journal of E-Health and Medical Communications (IJEHMC)*, v. 3, n. 4, p. 31–41, 2012. Disponível em: <http://www.igi-global.com/article/content/73705>. Cited 4 times on pages 22, 23, 76, and 77.

LUCK, S. J. *An introduction to the event-related potential technique*. [S.l.]: MIT Press, 2005. Cited on page 10.

MAGEE, R.; GIVIGI, S. A genetic algorithm for single-trial p300 detection with a low-cost eeg headset. In: *Systems Conference (SysCon), 2015 9th Annual IEEE International*. [s.n.], 2015. p. 230–234. Disponível em: <http://dx.doi.org/10.1109/SYSCON.2015.7116757>. Cited 2 times on pages 1 and 2.

MAGEE, R.; GIVIGI, S. A genetic algorithm for single-trial p300 detection with a low-cost eeg headset. In: *Systems Conference (SysCon), 2015 9th Annual IEEE International*. [s.n.], 2015. p. 230–234. Disponível em: <http://dx.doi.org/10.1109/SYSCON.2015.7116757>. Cited 4 times on pages 22, 23, 75, and 77.

MASON, S. G.; BIRCH, G. E. A general framework for brain-computer interface design. *IEEE Transactions on Neural Systems and Rehabilitation Engineering*, v. 11, n. 1, p. 70–85, 2003. Disponível em: <http://doi.ieeecomputersociety.org/10.1109/DASC.2009.72>. Cited 3 times on pages 2, 17, and 19.

MCFARLAND, D. J.; MINER, L. A.; VAUGHAN, T. M.; WOLPAW, J. R. Mu and beta rhythm topographies during motor imagery and actual movements. *Brain topography*, v. 12, n. 3, 2000. Disponível em: <http://link.springer.com/article/10.1023/A:1023437823106>. Cited on page 18.

MCFARLAND, D. J.; SARNACKI, W. A.; TOWNSEND, G.; VAUGHAN, T.; A, J. R. W. The P300-based brain–computer interface (BCI): Effects of stimulus rate. *Clinical Neurophysiology*, v. 122, n. 4, p. 731–737, 2011. Disponível em: <http://dx.doi.org/10.1016/j.clinph.2010.10.029>. Cited on page 1.

MELGES, D. B. *Aplicação de Técnicas de Detecção Objetiva nos domínios do tempo e freqüência ao EEG durante estimulação somato-sensitiva*. Tese (Doutorado) — Universidade Federal do Rio de Janeiro, 2009. Disponível em: <http://objdig.ufrj.br/60/teses/coppe_d/DaniloBarbosaMelges.pdf>. Cited 2 times on pages 11 and 12.

MOORE, M. M. Real-world applications for brain-computer interface technology. *Neural Systems and Rehabilitation Engineering, IEEE Transactions on*, v. 11, n. 2, p. 162–165, 2003. Disponível em: <http://www.ncbi.nlm.nih.gov/pubmed/12899263>. Cited on page 17.

MORALES, C.; HELD, C.; ESTEVEZ, P.; PEREZ, C.; REYES, S.; PEIRANO, P.; ALGARIN, C. Single trial p300 detection in children using expert knowledge and som. In: *Engineering in Medicine and Biology Society (EMBC), 2014 36th Annual International Conference of the IEEE*. [s.n.], 2014. p. 3801–3804. Disponível em: <http://dx.doi.org/10.1109/EMBC.2014.6944451>. Cited 4 times on pages 2, 22, 23, and 77.

MUGLER, E. M.; RUF, C. A.; HALDER, S.; BENSCH, M.; KUBLER, A. Design and implementation of a p300-based brain-computer interface for controlling an internet browser. *IEEE Transactions on Neural Systems and Rehabilitation Engineering*, v. 18, n. 6, p. 599–609, 2010. Disponível em: <http://dx.doi.org/10.1109/TNSRE.2010.2068059>. Cited on page 20.

MÜNSSINGER, J. I.; HALDER, S.; KLEIH, S. C.; FURDEA, A.; RACO, V.; HÖSLE, A.; KÜBLER, A. Brain painting: first evaluation of a new brain–computer interface application with als-patients and healthy volunteers. *Frontiers in Neuroscience*, v. 4, 2010. Disponível em: <http://www.ncbi.nlm.nih.gov/pmc/articles/PMC2996245/>. Cited on page 20.

MYERS, R. H.; MONTGOMERY, D. C.; VINING, G. G.; ROBINSON, T. J. *Generalized linear models: with applications in engineering and the sciences*. [S.l.]: John Wiley & Sons, 2012. v. 791. Cited 2 times on pages 38 and 39.

NICOLAS-ALONSO, L. F.; GOMEZ-GIL, J. Brain computer interfaces, a review. *Sensors*, v. 12, n. 2, p. 1211–1279, 2012. Disponível em: <http://www.mdpi.com/1424-8220/12/2/1211/pdf>. Cited 2 times on pages 16 and 17.

NIEDERMEYER, E.; SILVA, F. L. da. *Electroencephalography: Basic Principles, Clinical Applications, and Related Fields*. 5th. ed. [S.l.]: Lippincott Williams and Wilkins, 2004. ISBN 0781751268. Cited 7 times on pages 5, 7, 8, 9, 11, 12, and 17.

NOLAN, H.; WHELAN, R.; REILLY, R. B. Faster: Fully automated statistical thresholding for eeg artifact rejection. *Journal of Neuroscience Methods*, v. 192, n. 1, p. 152 – 162, 2010. Disponível em: <http://www.ncbi.nlm.nih.gov/pubmed/20654646>. Cited on page 8.

OLIVEIRA, A. S. B.; PEREIRA, R. D. B. Amyotrophic lateral sclerosis (ALS): three letters that change the people's life. For ever. *Arquivos de Neuro-Psiquiatria*, v. 67, p. 750 – 782, 2009. Disponível em: <http://www.ncbi.nlm.nih.gov/pubmed/19722069>. Cited on page 1.

PIRES, G.; NUNES, U.; CASTELO-BRANCO, M. Statistical spatial filtering for a p300-based bci: tests in able-bodied, and patients with cerebral palsy and amyotrophic lateral sclerosis. *Journal of neuroscience methods*, v. 195, n. 2, p. 270–281, 2011. Disponível em: <http://dx.doi.org/10.1016/j.jneumeth.2010.11.016>. Cited on page 15.

POLICH, J. On the relationship between EEG and P300: individual differences, aging, and ultradian rhythms. *International journal of psychophysiology*, v. 26, n. 1-3, p. 299–317, 1997. Disponível em: <http://www.sciencedirect.com/science/article/pii/S0167876097007721>. Cited on page 13.

POLICH, J. Updating p300: An integrative theory of p3a and p3b. *Clinical Neurophysiology*, v. 118, n. 10, p. 2128 – 2148, 2007. Disponível em: <http://www.ncbi.nlm.nih.gov/pubmed/17573239>. Cited on page 13.

REBSAMEN, B.; TEO, C. L.; ZENG, Q.; ANG, V.; BURDET, E.; GUAN, C.; ZHANG, H.; LAUGIER, C. Controlling a wheelchair indoors using thought. *IEEE Intelligent Systems*, v. 22, n. 2, p. 18–24, 2007. Disponível em: <http://dx.doi.org/10.1109/MIS.2007.26>. Cited on page 21.

RICCIO, A.; SIMIONE, L.; SCHETTINI, F.; PIZZIMENTI, A.; INGHILLERI, M.; BELARDINELLI, M. O.; MATTIA, D.; CINCOTTI, F. Attention and p300-based bci performance in people with amyotrophic lateral sclerosis. *Front Hum Neurosci 2013 Nov; 7*, v. 732, n. 2,906, 2013. Disponível em: <https://doi.org/10.3389/fnhum.2013.00732>. Cited on page 45.

ROSENFELD, J. P300 in detecting concealed information. In: VERSCHUERE, B.; BEN-SHAKHAR, G.; MEIJER, E. (Ed.). *Memory Detection: Theory and Application of the Concealed Information Test*. [S.l.]: Cambridge University Press, 2011. Cited on page 13.

ROWLAND, N.; MEILE, M.; NICOLAIDIS, S. *et al.* Eeg alpha activity reflects attentional demands, and beta activity reflects emotional and cognitive processes. *Science*, v. 228, n. 4700, 1985. Cited on page 7.

SALILLAS, E.; YAGOUBI, R. E.; SEMENZA, C. Sensory and cognitive processes of shifts of spatial attention induced by numbers: an erp study. *Cortex*, v. 44, n. 4, p. 406–413, 2008. Disponível em: <https://doi.org/10.1016/j.cortex.2007.08.006>. Cited on page 9.

SAUNDERS, M. G. Artifacts: activity of noncerebral origin in the eeg. In: KLASS, D. W.; DALY, D. D. (Ed.). *Current Practice of Clinical Electroencephalography*. [S.l.]: Raven Press, 1979. Cited on page 8.

SILVONI, S.; VOLPATO, C.; CAVINATO, M.; MARCHETTI, M.; PRIFTIS, K.; MERICO, A.; TONIN, P.; KOUTSIKOS, K.; BEVERINA, F.; PICCIONE, F. P300-based brain-computer interface communication: evaluation and follow-up in amyotrophic lateral sclerosis. *Frontiers in neuroscience*, v. 3, p. 1, 2009. Disponível em: <https://doi.org/10.3389/neuro.20.001.2009>. Cited on page 76.

SUR, S.; SINHA, V. K. Event-related potential: An overview. *Industrial Psychiatry Journal*, v. 18, n. 1, p. 70 – 73, 2009. Disponível em: <http://www.ncbi.nlm.nih.gov/pmc/articles/PMC3016705>. Cited 3 times on pages 9, 10, and 13.

SUTTON, S.; BRAREN, M.; ZUBIN, J.; JOHN, E. R. Evoked-potential correlates of stimulus uncertainty. *Science*, v. 150, p. 1187–1188, 1965. Disponível em: <http://www.ncbi.nlm.nih.gov/pubmed/5852977>. Cited on page 12.

TEPLAN, M. Fundamentals of EEG measurement. *Measurement Science Review*, v. 2, n. 2, p. 1–11, 2002. Disponível em: <http://www.measurement.sk/2002/S2/Teplan.pdf>. Cited 2 times on pages 5 and 7.

VALENS, C. *A really friendly guide to wavelets*. 1999. Disponível em: <http://agl.cs.unm.edu/~williams/cs530/arfgtw.pdf>. Cited 3 times on pages 34, 35, and 36.

VAREKA, L.; MAUTNER, P. Using the windowed means paradigm for single trial p300 detection. In: *Telecommunications and Signal Processing (TSP), 2015 38th International Conference on*. [s.n.], 2015. p. 1–4. Disponível em: <http://dx.doi.org/10.1109/TSP.2015.7296414>. Cited 3 times on pages 22, 23, and 77.

VENABLES, W. N.; RIPLEY, B. D. *Modern applied statistics with S-PLUS*. [S.l.]: Springer Science & Business Media, 2013. Cited 2 times on pages 37 and 38.

VIANA, S. S.; SCALZO, P. L.; MELGES, D. B. A variance-based approach to perform single-trial p300 detection. In: *Annals of the XXV Brazilian Congress on Biomedical Engineering*. [S.l.: s.n.], 2016. p. 1598–1601. Cited on page 32.

VIGáRIO, R.; JOUSMäKI, V.; HäMäLäINEN, M.; HARI, R.; OJA, E. Independent component analysis for identification of artifacts in magnetoencephalographic recordings. In: *Proceedings of the Neural Information Processing Systems*. The MIT Press, 1997. Disponível em: <http://dl.acm.org/citation.cfm?id=302596>. Cited on page 27.

W, S. E.; DONCHIN, E. A P300-based brain-computer interface: initial tests by ALS patients interfaces. *Clinical Neurophysiology*, v. 117, n. 3, p. 538–548, 2006. Disponível em: <http://www.ncbi.nlm.nih.gov/pubmed/16461003/>. Cited 3 times on pages 19, 20, and 75.

WOLPAW, J.; BIRBAUMER, N.; MCFARLAND, D.; PFURTSCHELLER, G.; VAUGHAN, T. Brain-computer interfaces for communication and control. *Clinical Neurophysiology*, v. 113, n. 6, p. 167–791, 2002. Disponível em: <http://doi.acm.org/10.1145/1941487.1941506>. Cited 4 times on pages 1, 16, 17, and 19.

WU, Q.; ZHANG, Y.; LIU, J.; SUN, J.; LI, J. Sparse optimal score based on generalized elastic net model for brain computer interface. In: *Information Science and Technology (ICIST), 2016 Sixth International Conference on*. [s.n.], 2016. p. 66–71. Disponível em: <http://dx.doi.org/10.1109/ICIST.2016.7483387>. Cited 3 times on pages 22, 24, and 77.

XIE, S.; WU, Y.; ZHANG, Y.; ZHANG, J.; LIU, C. Single channel single trial p300 detection using extreme learning machine: Compared with bpnn and svm. In: *Neural Networks (IJCNN), 2014 International Joint Conference on*. [s.n.], 2014. p. 544–549. Disponível em: <http://dx.doi.org/10.1109/IJCNN.2014.6889400>. Cited on page 2.

ZICKLER, C.; RICCIO, A.; LEOTTA, F.; HILLIAN-TRESS, S.; HALDER, S.; HOLZ, E.; STAIGER-SÄLZER, P.; HOOGERWERF, E.-J.; DESIDERI, L.; MATTIA, D. *et al.* A brain-computer interface as input channel for a standard assistive technology software. *Clinical EEG and Neuroscience*, v. 42, n. 4, p. 236–244, 2011. Disponível em: <http://eeg.sagepub.com/content/42/4/236.short>. Cited on page 21.

Appendix

APPENDIX A – Papers Published During the Master's Degree Course

During the Master's Degree Course, the following paper was published in the XXV Brazilian Congress on Biomedical Engineering:

1. VIANA, S. S.; SCALZO, P. L.; MELGES, D. B. A Variance-based Approach to Perform Single-Trial P300 Detection. In: XXV Brazilian Congress on Biomedical Engineering. p. 1598-1601, 2016.

The paper can be seen in: <https://www.researchgate.net/profile/Sadraque_Viana/publication/311847543_A_Variance-based_Approach_to_Perform_Single-Trial_P300_Detection>